

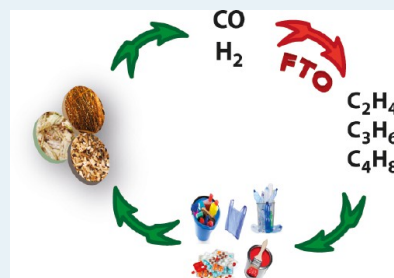
Catalysts for Production of Lower Olefins from Synthesis Gas: A Review

Hirsa M. Torres Galvis and Krijn P. de Jong*

Inorganic Chemistry and Catalysis, Utrecht University, Universiteitsweg 99, 3584 CG Utrecht, The Netherlands

ABSTRACT: C_2 to C_4 olefins are traditionally produced from steam cracking of naphtha. The necessity for alternative production routes for these major commodity chemicals via non-oil-based processes has driven research in past times during the oil crises. Currently, there is a renewed interest in producing lower olefins from alternative feedstocks such as coal, natural gas, or biomass, in view of high oil prices, environmental regulations, and strategies to gain independence from oil imports. This review describes the major routes for the production of lower olefins from synthesis gas with an emphasis on a direct or single step process, the so-called FTO or Fischer–Tropsch to olefins process. The different catalysts for FTO are outlined and compared, and the key issues and requirements for future developments are highlighted. Iron-based catalysts are prevailing for FTO, and reproducible lower olefin selectivities of 50 wt % of hydrocarbons produced have been realized at CO conversions higher than 70% for 60 to 1000 h on stream. Remarkably the high selectivity to lower olefins has been achieved over a broad range of process conditions (P, T, H_2/CO ratio, GHSV). A major challenge for further development and application of FTO catalysts is the suppression of carbon lay-down to enhance catalyst lifetime and to preserve their physical integrity under demanding reaction conditions.

KEYWORDS: Fischer–Tropsch, light olefins, synthesis gas, FTO, supported catalysts, bulk catalysts, ethylene, propylene



1. INTRODUCTION

1.1. Lower Olefins. Ethylene, propylene, and butylenes are key building blocks in the chemical industry. Throughout this review we refer to C_2 – C_4 olefins as lower or light olefins. These base chemicals are among the organic chemicals with the largest production volumes worldwide (Table 1). Their broad spectrum of derivatives result in a very diverse end market ranging from packing materials and synthetic textiles to antifreezing agents, solvents, and coatings.

Ethylene is the largest-volume petrochemical produced worldwide. It is used to produce intermediate chemicals of high importance in industry such as ethyl benzene, ethylene oxide, and ethylene dichloride, which were listed, along with ethylene, in the top 30 highest volume chemicals in the United

States in 2000.² The major chemicals derived from ethylene and their derivatives are shown in Figure 1. Ethylene is mainly used by the plastics industry. In 2010, approximately 61% of the total consumption of ethylene was for production of polyethylene in the Western European countries (Figure 2). Ethylene is also used in the production of other plastics such as polystyrene (PS), polyethylene terephthalate (PET), and polyvinyl chloride (PVC), which are widely used in the packaging, textile, and construction industries.

Commercial ethylene production is mainly based on steam cracking of a broad range of hydrocarbon feedstocks. In Europe and Asia, ethylene is obtained mainly from cracking of naphtha, gas oil, and condensates, while in the U.S., Canada, and the Middle East ethylene is produced by cracking of ethane and propane. Naphtha cracking is the major source of ethylene worldwide; however, gas cracking has been gaining importance in recent years.

Propylene is a versatile petrochemical which has even more derivatives than ethylene. However, the tremendous growth of polypropylene consumption over the past 15 years has been the main driver of the large increase of the demand of propylene. In 2010, more than 55% of propylene consumption was dedicated to the production of polypropylene in the Western European countries. Approximately 13% of the propylene was used in the production of propylene oxide, which is a chemical precursor for the synthesis of propylene glycol and polyols. The rest of

Table 1. Production of Organic Chemicals in 2010 in Thousands of Metric Tons¹

	U.S.A.	Asia ^a	China	Europe
ethylene	23975	18237	14188	19968
propylene	14085	14295	na ^b	14758
ethylene dichloride	8810	3222 ^c	na	1323
benzene	6862 ^d	10889	5530	5107
ethyl benzene	4240	na	na	1226
cumene	3478	na	na	na
ethylene oxide	2664	845 ^c	na	2619
butadiene	1580 ^e	2715	na	2020
methanol	na	na	15740	na

^aJapan, South Korea, and Taiwan. ^bInformation not available. ^cJapan only. ^dThousands of liters. ^e1,3-Butadiene rubber grade.

Received: May 13, 2013

Revised: July 3, 2013

Published: July 8, 2013

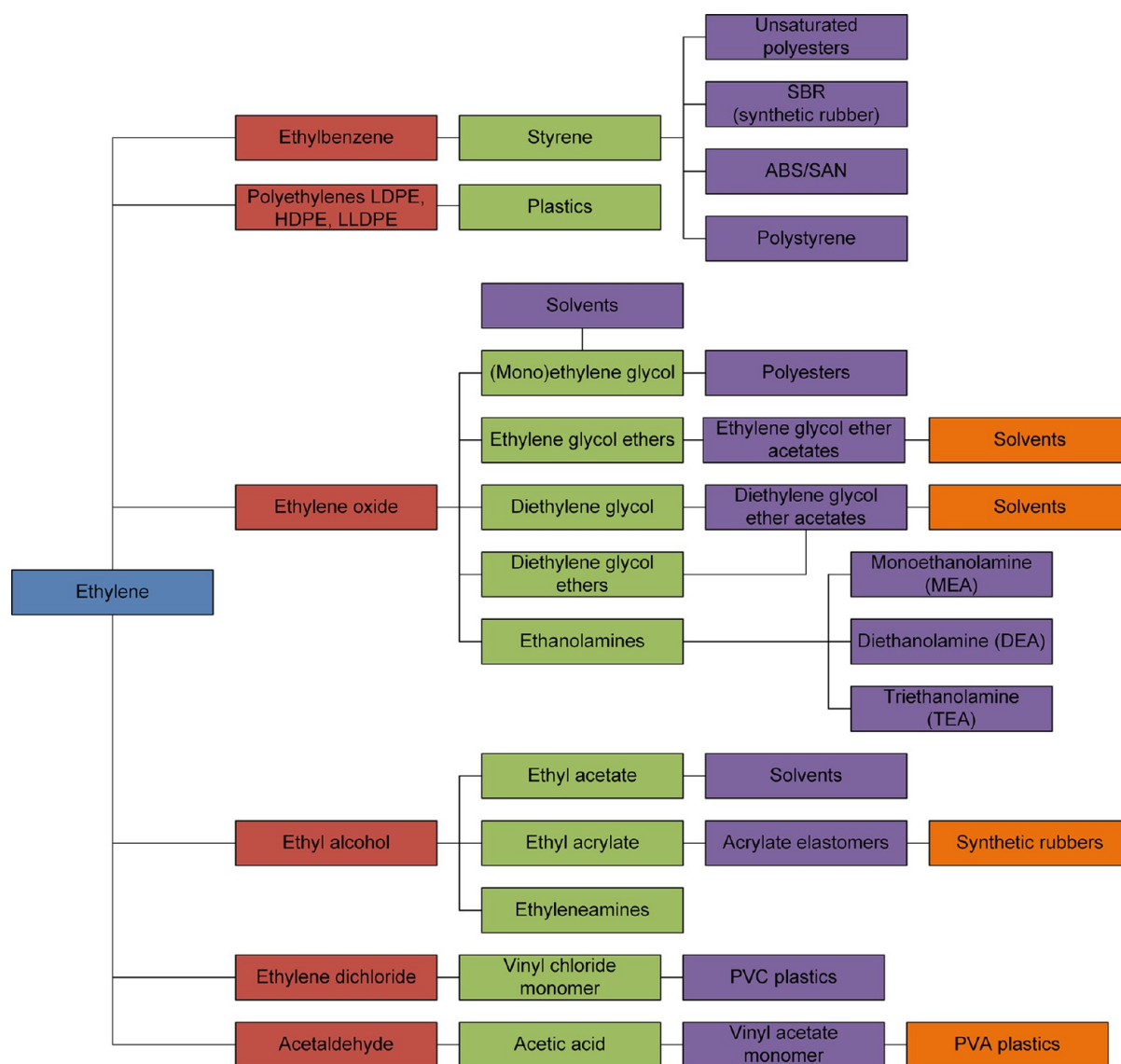


Figure 1. Ethylene and its derivatives.

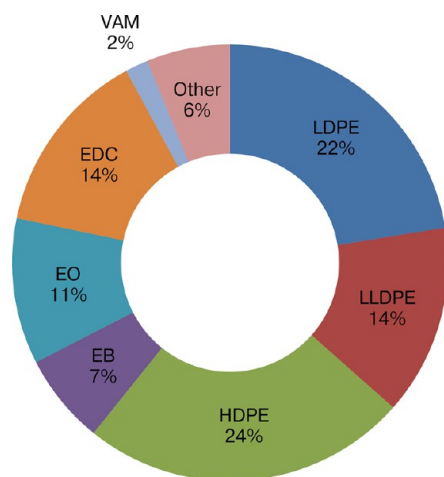


Figure 2. Ethylene consumption over different products in the Western European countries. LDPE: low-density polyethylene. LLDPE: linear low-density polyethylene. HDPE: high-density polyethylene. EB: ethyl benzene. EO: ethylene oxide. EDC: ethylene dichloride. VAM: vinyl acetate monomer. Statistics of 2010.³

the production was used in the synthesis of cumene (about 8%), acrylonitrile, isopropyl alcohol, and many other industrially relevant chemicals.³

Traditionally, propylene is produced as a byproduct of steam cracking of naphtha for ethylene production or it is recovered from refinery processes, especially from fluid catalytic cracking (FCC). During steam cracking it is possible to tune the propylene/ethylene ratio by varying the severity of the cracking process. A low severity cracking process yields less ethylene and more byproducts. Although the normal condition is moderately high severity cracking to achieve ethylene maximization, the necessity to increase the production of high value byproducts, such as propylene, may dictate lowering the severity during short-term optimization.

Refinery propylene is primarily derived from FCC, visbreaking/thermal cracking, and coking. For all of these processes propylene is obtained as a diluted stream in propane. FCC-derived propylene accounts for approximately 30% of the global supply, and this percentage tends to increase as the steam cracking-derived propylene decreases as a result of the growth of ethylene production from ethane-based cracking.⁴ In

recent years, the production of propene via dehydrogenation of propane (PDH) has grown in view of the availability of low-price propane in shale gas.⁵

The C₄ olefins fraction is composed of butadiene, isobutylene, and *n*-butenes which are used in fuel and chemical applications. Butadiene is mainly used as raw material for the production of different types of synthetic rubber (SBR, polybutadiene rubber, etc.). These synthetic rubbers are in high demand all over the world, especially in Asia, for the manufacture of finished goods in the electronics and automotive sectors. Butadiene is also used for the production of ABS (acrylonitrile–butadiene–styrene), SB (styrene–butadiene) copolymer latex and block copolymers, and nitrile rubbers (NBR).

One of the most important applications of butylenes is in the fuel industry, accounting for approximately 85% of butylenes' world production. They are used for the production of gasoline alkylate, polymer gasoline, and dimersol, which are gasoline blending components. Isobutylene is a raw material for the synthesis of methyl *tert*-butyl ether (MTBE) and ethyl *tert*-butyl ether (ETBE), which are used as octane enhancers, and for the production of isooctane by dimerization and subsequent hydrogenation.

n-Butenes have a smaller chemical market compared with butadiene and isobutylene. They are used as comonomers for polyethylene, for the production of *sec*-butyl alcohol, which is a raw material in the synthesis of MEK (methyl ethyl ketone), and for the synthesis of higher olefins.

Approximately 95% of butadiene world production is a byproduct of the steam cracking of naphtha and gas oil for the production of ethylene and propylene. Butadiene is then recovered from the C₄ cracker stream by extractive distillation. Other processes for the production of butadiene involve further processing of the C₄ stream, e.g., recycle cocracking with and without selective or full dehydrogenation.

1.2. Alternative Feedstocks. The constantly growing demand for lower olefins has caused the global production capacity to double over the past 15 years. During 2008 and 2009, ethylene demand decreased due to the slow global economic growth; nevertheless, analysts predict that the demand will grow after 2012 (Figure 3).

It is expected that new steam crackers will provide sufficient ethylene to meet the growing demand. Propylene production

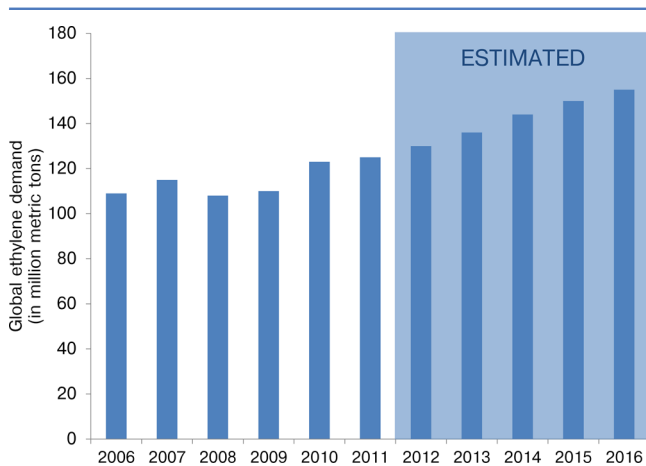


Figure 3. Ethylene demand in the period 2006–2011. Forecast for the period 2012–2016. Source: CMAI.

will increase as well; however, according to experts the production capacity will be insufficient to cover the demand.⁶

The growth of the demand for lower olefins will inevitably increase the demand for the feedstocks required in the petrochemical industry. With the recent high oil prices, research has been directed to the development of processes based on alternative feedstocks for the production of lower olefins.

Apart from high oil prices, there are some other drivers in the search for alternative routes and feedstocks:

- The production of lower olefins via steam cracking is one of the ten most energy-consuming processes of the chemical and petrochemical industry.⁷
- There is a growing awareness of the depletion of conventional oil reserves. Some analysts suggest that oil consumption will surpass the discovery of new reserves followed by the depletion of known reserves.⁸
- The oil contained in unconventional reserves is heavy oil in the case of so-called oil sands. The extraction and upgrading of unconventional oil currently may involve higher costs and higher CO₂ emissions in comparison with conventional oil.⁹
- There is a pressing necessity to decrease CO₂ emissions.¹⁰ Feedstocks such as biomass have lower net CO₂ contribution.¹¹
- Many countries, among them Japan, China, and Brazil, are searching for alternatives to reduce their reliance on imported crude oil and refined products.

Several processes have been developed in an attempt to solve one or more of the challenges encountered by the lower olefins industry. These processes are based on alternative feedstock such as coal, natural gas, or biomass.

Although coal has long been used as a feedstock for the chemical industry, for instance, for the production of acetylene via the carbide process and for the synthesis of ammonia, in times of abundant low-cost oil and gas, its role diminished.

The rapid increase of energy demand, the high oil and gas prices, and the strategic drive of coal-rich countries to reduce their dependence on imported crude oil have led to reconsider coal as a primary feedstock for the production of chemicals.

Countries with large coal reserves, such as China, are very active in the research, development, and implementation of coal-based projects such as the transformation of syngas to olefins via methanol synthesis (MTO) or via dimethyl ether or SDTO process (syngas via dimethyl ether to olefins). However, there are some challenges in the great potential of the coal-to-olefins industry. Coal gasification generates excess CO₂ that has to be removed from the synthesis gas and discharged from the plant. The environmental pressure to reduce CO₂ emissions may bring about CO₂ sequestration technologies that have to be implemented before coal-based processes are established worldwide.

Biomass gasification has potential as a source for hydrocarbon products in view of feedstock flexibility and the possibilities to reduce net CO₂ emissions.^{12–15} The use of biomass for the production of lower olefins might benefit from low feedstock costs and tax incentives. However, the potential for cost reduction in light olefins production is limited by the cost of collection and transportation of biomass in large-scale applications and the production of synthesis gas.

The use of biomass is mainly encouraged by its carbon-neutral nature. Biomass may be transformed through pyrolysis

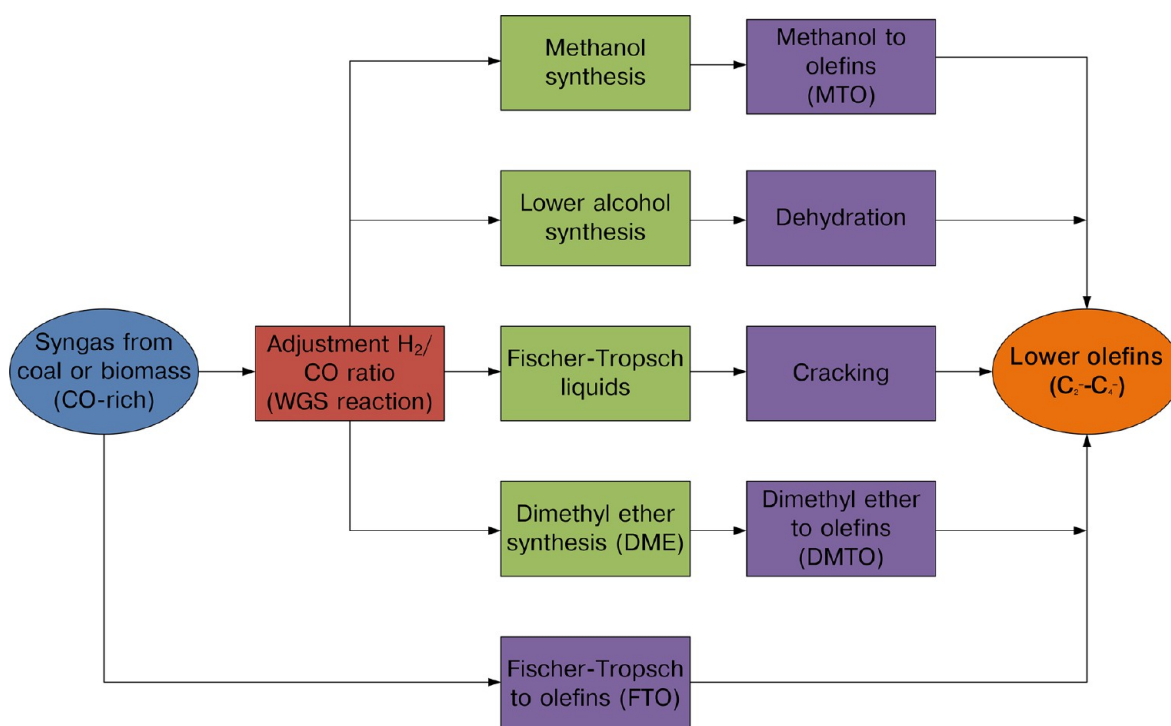


Figure 4. Processes for the transformation of CO-rich synthesis gas into lower olefins.

to achieve high energy density and then converted to syngas. The syngas obtained from biomass is CO-rich and in general contains several impurities, as is the case for coal-based syngas. The syngas derived from these sources requires extensive purification to remove contaminants, such as sulfur, that are detrimental for the catalysts used in syngas transformation processes. For most conversion processes, the H_2/CO ratio needs to be adjusted by means of the water gas shift reaction (WGS). After purification and tuning the H_2/CO ratio, syngas can be used for the production of chemicals and fuels.

With the recent discovery of large shale gas reserves in the U.S.,^{16,17} new possibilities are open for the transformation of natural gas to olefins. Wet shale gas can be directly fed to ethane crackers to produce ethylene, while dry shale gas can be used for the production of syngas and thus be transformed directly or indirectly to lower olefins.

The increased availability of natural gas from shale deposits has produced a major shift in the feedstocks used for the production of ethylene in U.S., and consequently it has affected the propylene and butadiene markets. The use of ethane as feedstock for the crackers instead of naphtha results in a tighter supply of C_3 and C_4 olefins, and it might increase the prices for those chemicals in the future.^{5,18} These issues have also opened opportunities for alternative processes for the production of propylene and butylenes.

Large shale gas reserves have been found not only in U.S. but also in other countries such as China, which holds the largest technically recoverable reserves.¹⁹ The exploitation of shale gas for energy purposes and for the production of lower olefins is expected to increase dramatically in the years to come in spite of some environmental concerns related to its extraction²⁰ and the high costs involved in the production of shale gas.²¹

2. PRODUCTION OF LOWER OLEFINS FROM SYNTHESIS GAS

Some of the alternative processes for the production of lower olefins are dehydrogenation of lower alkanes, syngas-based processes, and specific processes for target products such as the production of ethylene via dehydration of ethanol derived from renewable sources or propylene synthesis via dehydrogenation of propane obtained as a byproduct of biodiesel production.

Figure 4 displays the different conversion processes that use coal or biomass-based syngas as feedstock. The same scheme applies for H_2 -rich syngas although, in that case, the step for the adjustment of the H_2/CO ratio is not necessary. The processes for the production of lower olefins via syngas can be divided into two main groups: indirect processes, which require the synthesis of an intermediate such as methanol or dimethyl ether, and direct processes.

2.1. Indirect Processes. Several indirect processes for the conversion of syngas to lower olefins have been developed in view of the selectivity restriction posed by the Anderson–Schulz–Flory product distribution that governs the Fischer–Tropsch synthesis.^{22–25} The methanol-to-olefins process (MTO) has been developed and commercialized in places where the technology has an economical advantage over naphtha cracking and other natural gas conversion processes.

Mobil synthesized the ZSM-5 zeolite and used it for the methanol-to-gasoline process (MTG).²⁶ Later, the MTO process was developed by UOP/Hydro to produce a mixture of C_2 – C_4 olefins from methanol using a zeolite-based catalyst. The main product of MTO is ethylene when the process is performed using a SAPO-34 catalyst. The MTO UOP/Hydro process produces up to 90% of light olefins from methanol, but the SAPO-34 catalyst can be rapidly deactivated (in the order of minutes to hours) by coke formation, depending on reaction conditions and crystal size.²⁷

High selectivities to propylene have not been reported for the MTO process using SAPO-34.²⁸ For this reason, the methanol-to-propylene (MTP) process was developed by Lurgi to selectively produce propylene obtaining gasoline, fuel gas, and LPG as byproducts. The ZSM-5-based Lurgi process produces up to 70% propylene from methanol via recycling of byproducts.²⁹

Liu et al.²² reported on a pilot plant for MTO using two reactors: the first reactor contained γ -Al₂O₃ to dehydrate methanol to dimethyl ether (DME), and the second one used ZSM-5 for the conversion of DME to light olefins. They obtained a C₂–C₄ olefin selectivity of 85 wt % (C₂H₄, 24 wt %; C₃H₆, 40 wt %) with a methanol conversion of 100%. The catalyst showed a good stability during the 1500 h of the test.

Another indirect process that has been developed is the dimethyl ether-to-olefins process (DMTO) that is also known as SDTO (syngas-via-dimethyl ether-to-olefins) or simply DTO. In principle this process could be more efficient than MTO as the synthesis of dimethyl ether (DME) from syngas has more favorable thermodynamics in comparison with methanol synthesis. The process uses two types of catalysts: in a first reactor, the DME synthesis is carried out using a metal–acid bifunctional catalyst, and the DME conversion reaction is performed using a SAPO-34 catalyst in a second reactor. Liu and co-workers²² reported a C₂–C₄ olefin selectivity of 90 wt % (C₂H₄, ~60 wt %; C₃H₆, ~20 wt %) at a DME conversion of 100%, using a Cu–Zn/ZSM-5 catalyst for the conversion of syngas to DME and a metal-modified SAPO-34 type of molecular sieve for the conversion of DME to lower olefins. Selectivities to other products were not reported. The SAPO-type catalyst had to be regenerated by coke burnoff. The catalyst retained its performance after regeneration and only showed a small decrease in relative crystallinity in the presence of water.³⁰ It has been stated that DMTO should be closely related to MTO because of the fast conversion equilibrium that occurs among methanol, DME, and water;²⁸ this has been observed as well by Liu et al. when they used methanol instead of DME on their modified SAPO-type catalyst obtaining similar selectivities.²²

Zhao et al.²⁸ investigated the synthesis of light olefins over modified H-ZSM-5 catalysts using DME as feed. They obtained high C₂–C₄ olefin selectivities (up to 75% C) with preferential formation of propylene (~45% C) using zirconia-modified H-ZSM-5.

Some of other indirect processes for the production of lower olefins from synthesis gas that have been reported are as follows:

1. The Texaco process.³¹ This process consists of two stages: in the first step, syngas is converted into carboxylic acid esters in a homogeneous reaction in the presence of a ruthenium catalyst promoted with quaternary phosphonium salts. The second stage involves the pyrolysis of the aliphatic carboxylic acid esters to alkenes and the parent acid. Product selectivity can be tailored depending on the feed to obtain ethylene or propylene selectivities up to 55%.
2. A process developed by Dow Chemical Company to transform syngas into a mixture of lower alcohols (C₁–C₅) using molybdenum sulfides. The alcohol mix can be subsequently dehydrated to produce lower olefins.
3. The production of lower olefins from FT liquids.³² Hydrocarbons that are produced through the Fischer–

Tropsch reaction route can be transformed into C₂–C₄ olefins through cracking and upgrading using traditional petrochemical processes.

All indirect processes involve more than one step which generates additional costs in terms of equipment and energy consumption. However, processes with high selectivities to ethylene such as MTO or DMTO, or highly selective toward propylene like MTP, can be of great interest for the production of polyethylene or polypropylene in remote areas not linked to chemical complexes.^{33,34}

2.2. Direct Processes. The direct conversion of syngas into lower olefins via the Fischer–Tropsch synthesis of the Fischer–Tropsch to olefins (FTO) process is an interesting option compared to cracking of FT liquids, MTO, or DMTO.³⁴ The idea of following a direct route for the synthesis of lower olefins from synthesis gas has been considered for more than 50 years, and many references can be found in the literature about catalytic systems that might be suitable for this application.^{24,25,35}

Figure 5 represents the output of research publications and industrial patents on the direct Fischer–Tropsch synthesis of

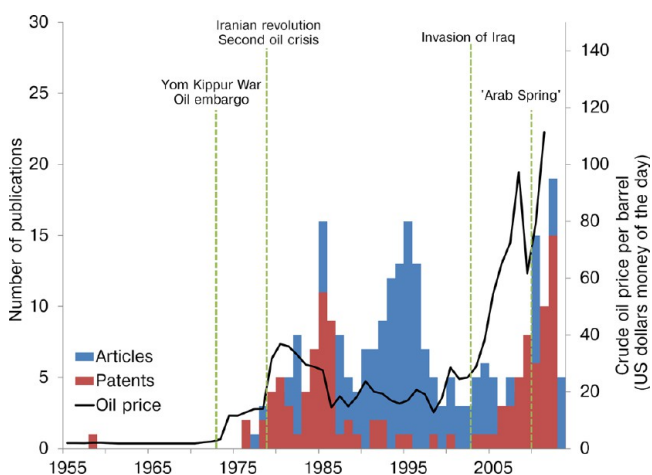


Figure 5. Scientific papers and patents on the direct production of lower olefins via Fischer–Tropsch³⁶ (bars) in 1955–2013 in relation to the oil price³⁷ (solid line).

lower olefins since 1955. The increase in the number of publications in this subject was preceded by periods where oil prices reached peak values. It is also clear that oil prices are strongly dependent on geopolitical issues as depicted in Figure 5.

It is interesting to observe for instance how the number of patents on the direct production of light olefins from syngas reached maximum values after the oil embargo of 1973 and the second oil crisis in 1979. The shortage and the consequent high cost of oil for the production of light olefins via naphtha cracking increased the urge to develop alternative routes to produce these valuable commodity chemicals via syngas-based processes.

After oil prices dropped to lower levels, between 1987 and 2003, the number of patents on the topic decreased but academic research related to the catalysts and the process was still very active. During this period the scientific publications were mostly dedicated to the influence of chemical promoters and supports on C₂–C₄ olefins selectivity and to the

optimization of process conditions to maximize the activity and selectivity toward the target products.

After the invasion of Iraq in 2003 oil prices rose steeply, renewing the interest of chemical and petrochemical companies on more efficient catalysts and processes to produce lower olefins using natural gas, coal, or biomass as feedstock. Once more in 2010, the oil prices increased dramatically caused by political instability in many oil-producing countries in the Middle East.

Therefore countries such as China and the U.S. with large reserves of natural and shale gas or coal are taking the lead on the research and development of direct processes for the production of C_2 – C_4 olefins to ensure a reliable supply of these bulk chemicals and to achieve independence from oil imports. Figure 6 shows the 10 countries with the highest number of research papers and patents on catalysts for the production of lower olefins via Fischer–Tropsch.

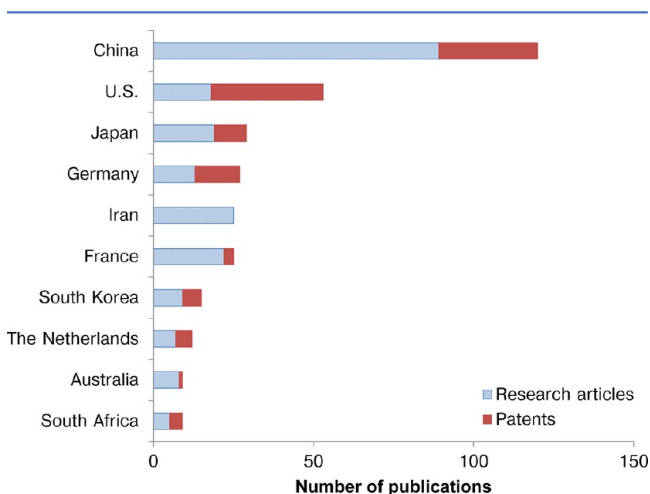


Figure 6. Number of publications on the direct production of lower olefins from synthesis gas from 1955 to 2013³⁶ (Fischer–Tropsch only, top 10 countries).

Despite of the number of publications on the direct production of lower olefins via the Fischer–Tropsch reaction, there has been no commercial application for this process in view of the low C_2 – C_4 olefins selectivity, low mechanical or chemical stability, or high methane production of some of the catalysts proposed up to now.

Researchers have developed different catalytic systems based on metals that exhibit CO hydrogenation activity. Among these metals only iron, cobalt, nickel, and ruthenium have been found to be sufficiently active for their application.³⁸ From the commercial standpoint only Fe and Co are used as they are more readily available and less expensive compared to ruthenium. Ni is very active as well, but it produces much more methane than Co or Fe and it forms volatile carbonyls at the reaction conditions at which FT plants operate, resulting in continuous loss of the metal. Other metals with moderate FT activity are Rh and Os. The products obtained from FT synthesis when using Rh as catalyst contain large fractions of oxygenates. Mo has also shown some FT activity in the presence of H_2S , but it was found to be less active than Fe. Cr has also been investigated as a possible FT catalyst, but its activity is even lower than Mo.

It has been found that the properties of the FT active metals can be modified by adding chemical promoters to improve

selectivity to light olefins or to enhance catalytic activity. Improvements on the mechanical stability of the catalysts might be achieved by addition of structural promoters whereas the surface area of the active metal can be extended by dispersing it on a support or carrier material. The different catalytic systems developed for the FTO process are discussed more in detail in section 3.

To the best of our knowledge, there are no other direct syngas transformation routes to produce lower olefins apart from FTO. Some researchers have designed hybrid processes that use one reactor with two different catalysts such as the development reported by Arakawa et al.³⁹ In this process the upper part of the catalyst bed consisted of a Rh–Ti–Fe–Ir/ SiO_2 catalyst to produce ethanol and the lower part contained H-silicalite for alcohol dehydration. This process produced approximately 45% C of ethylene while propylene and butylenes were produced in negligible amounts. Although selectivity to ethylene was high, the selectivity to methane was near 33% C. Another example is the composite catalyst developed by Denise et al.⁴⁰ where a physical mixture of a methanol catalyst (Cr_2O_3/ZnO) and dealuminated mordenite produced a mixture of light hydrocarbons (alkenes and alkanes in the C_1 – C_5 range).

Other examples of hybrid processes involve the use of a Fischer–Tropsch catalyst to produce hydrocarbons from syngas and further cracking of the products in a second catalyst bed containing a zeolite.^{41,42} Park et al.⁴¹ used a precipitated Fe–Cu– Al_2O_3 catalyst promoted with potassium for the FT synthesis while cracking of the C_{5+} products was performed on ZSM-5. Using this dual bed reactor they obtained a C_2 – C_4 olefins selectivity of 41% C with a low methane production (10%) under high CO conversions (320 °C, 10 bar, and $H_2/CO = 2$). Although it could be expected that the stability of the zeolite would be compromised by the presence of water during reaction, Lee et al.⁴² pointed out that ZSM-5 maintained its hydrothermal stability and activity at least during 100 h time on stream.

3. FISCHER–TROPSCHE TO OLEFINS PROCESS (FTO)

The Fischer–Tropsch synthesis is the reaction of CO and H_2 in the presence of an active catalyst to produce hydrocarbons and alcohols. Due to the nature of the reaction, which may be considered as a surface polymerization reaction, the product stream consists of a range of products instead of a single component. Although the mechanism of the Fischer–Tropsch reaction has been a matter of study for several years, it has not been completely elucidated yet. However, it is widely accepted that the reaction proceeds through a surface carbide mechanism which is shown as a simplified scheme in Figure 7.

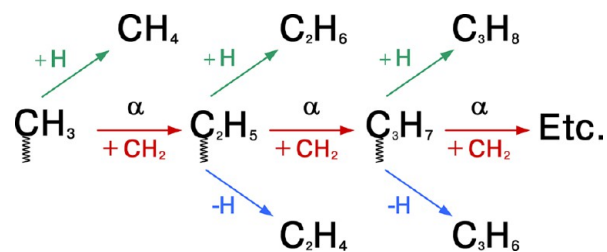


Figure 7. Fischer–Tropsch reaction mechanism (surface carbide mechanism).

The product distribution can be predicted using the Anderson–Schulz–Flory (ASF) model that depends on the chain growth probability α . Different factors have an influence on the alpha parameter such as process conditions, type of catalyst, and chemical promoters.⁴³ The ASF product distribution as a function of α is depicted in Figure 8.

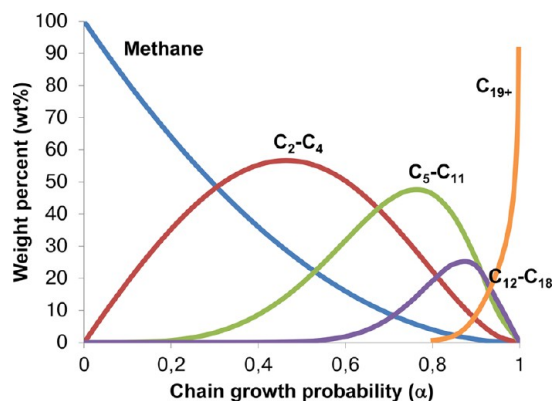


Figure 8. Anderson–Schulz–Flory (ASF) model for the prediction of product distribution.

Since the Fischer–Tropsch reaction has been known for almost a century, there is a vast amount of information related to the fundamentals of the reaction, the industrial process, and the FT catalysts, which has been covered in several comprehensive reviews.^{38,44–48} Other more specific reviews involve the preparation, application, and deactivation of iron,^{43,49,50} cobalt,^{51–53} and nickel⁵⁴ catalysts in the traditional Fischer–Tropsch process for the production of fuels. For this reason, we will not discuss the general aspects of the Fischer–Tropsch reaction or traditional FT catalysts but we rather focus on the Fischer–Tropsch synthesis of lower olefins or FTO and the catalysts for that purpose.

The primary aims of FTO are to maximize lower olefins selectivity, to reduce methane production, and to avoid the formation of excess CO₂. According to the ASF model, the maximum selectivity toward C₂–C₄ olefins is achieved with an alpha value between 0.4 and 0.5. One of the most efficient ways of shifting product selectivity to low alpha values is by increasing reaction temperature. However, a decrease on the chain growth probability results in an increase of methane selectivity as indicated by the ASF product distribution. This effect was long considered a major restriction for the industrial application of the direct conversion of syngas into lower olefins via the Fischer–Tropsch synthesis.^{24,25} Negative deviations of the ASF model for methane selectivity have been observed for iron-based catalysts.^{34,55} Schwab et al.³⁴ proposed that Fe catalysts possess different catalytic sites, some in charge of C–C coupling for the growth of the carbon chain and others responsible for methane formation. According to Schwab, these catalytic sites can be modified independently and controlled by addition of promoters. Torres Galvis et al.⁵⁶ ascribed the negative deviations of methane selectivity of Na/S-promoted iron catalysts to selective blockage of hydrogenation sites. They put forward that sulfur restricts the termination of carbon chain growth through hydrogenation thus favoring the β -hydride abstraction termination pathway. This proposal not only explains the lower methane selectivity but also the higher light olefins selectivity observed when iron catalysts were promoted with low amounts of sulfur.

The vast majority of the catalysts suggested for FTO contain iron. In comparison to cobalt, iron is less expensive, it has a lower activity, Fe Fischer–Tropsch products have a higher olefin content, as iron is less reactive to secondary hydrogenation reactions, and it displays lower methane selectivity at the high temperatures necessary to drive alpha to lower values. In view of their high water gas shift (WGS) activity, iron catalysts are an attractive option for the conversion of CO-rich syngas derived from coal or biomass because an additional H₂/CO ratio adjustment step is not necessary. Many catalyst formulations containing iron or other FT-active metals have been proposed for the synthesis of light olefins from synthesis gas. In this review we have divided these catalytic systems into two major groups: bulk or unsupported catalysts, including those materials with structural promoter content below 50 wt %, and supported catalysts.

Researchers in the field use different ways to present their catalytic data. The product selectivity for iron-based catalysts is generally reported excluding CO₂. Selectivity can be expressed based on weight (wt %: g of a product \times 100/g of hydrocarbons), molar-based (moles of a product \times 100/total moles of hydrocarbons) or carbon-based (% C: carbon atoms in a product \times 100/total carbon atoms present in hydrocarbons). The conversion of CO can be reported as total CO conversion (including CO₂) or CO conversion to hydrocarbons. Some other authors prefer to mention syngas conversion (CO + H₂) instead of CO conversion. In the following sections, product selectivity and CO conversion will be expressed as a percentage (%). The specific details on the choice of the researchers to report their results can be found in the summary tables (Tables 3 and 4).

3.1. Bulk or Unsupported Iron Catalysts. South Africa possesses large coal deposits and limited exploitable oil reserves. For this reason, this country has done its utmost to become independent from oil imports. In view of this necessity, the South African government issued a license to start the oil-from-coal project after the Second World War. Since 1955 SASOL has produced chemicals and gasoline using the so-called Synthol process.⁵⁷ The main aim of this process is to produce liquid fuels although lower olefins are also obtained depending on the operating conditions and the type of catalysts. The product selectivities obtained by SASOL with the low temperature (LTFT) and the high temperature (HTFT) processes is shown in Table 2.

The catalyst used for the HTFT process in fluidized bed reactors is a fused catalyst containing iron oxide and structural

Table 2. Fischer–Tropsch Products of Iron-Based Catalysts³⁸

	LTFT slurry reactor, T = 240 °C, 20 bar	HTFT fluidized bed reactor, T = 340 °C, 20 bar
% selectivities (C atom basis)		
methane	4	8
C ₂ –C ₄ paraffins	2.5	6
C ₂ –C ₄ olefins	6	24
C ₅ –C ₆	7	16
C ₇₊	76.5	41
water-soluble oxygenates	4	5
α	0.95	0.70

Table 3. Unsupported Catalyst for the Fischer–Tropsch to Olefins Process^a

catalyst: elements present	T (°C)	P (bar)	H ₂ /CO (molar)	CO convn (%)	CH ₄ (wt %)	C ₂ –C ₄ olefins (wt %)	CO convn to CO ₂ (%)	ref
Fe–Mn	350	15	2	96	30	52	nr	Wang et al. ²³
Fe–V–Zn–K	320	10	1	85 ^b	12	59	nr	Büssemeier et al. ⁵⁹
Fe–Mn–Zn–K	320	10	1	86 ^b	10	71	nr	Büssemeier et al. ⁵⁹
Fe–Ti–Zn–K	340	10	1	87 ^b	10	75	nr	Büssemeier et al. ⁶⁰
Fe–Ti–Zn–K	250	2.5	1	45 ^b	20	68	nr	Roy et al. ⁶¹
La–K–Mn–Fe	280	11	2	14	10	70	30	Goldwasser et al. ⁶²
Fe–Cu–Al (sol–gel)	300	10	2	96	7 ^c	21 ^c	40	Kang et al. ⁶⁴
Fe–Au–K	360	10	2	97	16	39	31	Vielstich et al. ⁶⁵
Fe carbonyl–Na	340	23	1	98	15 ^d	44 ^d	nr	Hoffer et al. ⁶⁶
(Co _{0.73} Fe _{0.27}) _{0.58} [Co _{0.69} Fe _{2.31} O ₄]	250	10	1	5	34	52	15	Tihay et al. ⁶⁷
(Co _{0.95} Fe _{0.05}) _{0.62} [Co _{0.31} Fe _{2.69} O ₄]	230	10	1	2	25	36	25	Tihay et al. ⁶⁸
Fe/Mn/S	350	1	1	<5	28 ^d	45 ^d (C ₂)	nr	Van Dijk et al. ⁶⁹
0.59 g of Na/0.12 g of S/100 g of Fe	330	20	4	41 ^b	9 ^d	39 ^d	nr	Crous et al. ⁷⁰
0.8 g of K/0.2 g of S/100 g of Fe	360	40	4	12 ^b	12 ^d	37 ^d	nr	Crous et al. ⁷⁰
Fe–Mn poisoned with H ₂ S feed	450	1	2	18	5–7 ^d	60 ^{d,e}	nr	Hadadzadeh et al. ⁷¹
Fe–Mn	300	1	1	10	44 ^c	26 ^c	~50	González-Cortés et al. ⁷²
Fe–Co–Mn	300	1	1	60	34 ^c	25 ^c	~50	González-Cortés et al. ⁷²
Fe–Co	450	1	4	85	nr	54 ^{d,e}	nr	Mirzaei et al. ⁷³
Fe–Co–Si	450	1	4	92	nr	65 ^{d,e}	nr	Mirzaei et al. ⁷³
Fe–Co–Si–K	450	1	4	88	nr	64 ^{d,e}	nr	Mirzaei et al. ⁷³
Fe–Co–K	260	1	2	64	10 ^d	54 ^d	5	Feyzi et al. ⁷⁴
Mn–Fe	285	10	0.7	53	7	52	nr	Kölbel et al. ⁷⁵
Fe–Mn	298	12	0.6	30 ^b	12	29	nr	Deckwer et al. ⁷⁶
Fe–Mn–K	305	21	1	92	10	34	44	Soled et al. ⁷⁷
Fe–Mn	300	2.5	1	nr	44	75 ^f	nr	Hutchings et al. ⁷⁸
Fe–Mn	300	6	1	36	14	15 ^e	nr	Copperthwaite et al. ⁷⁹
Co–Mn	190	3.5	1	24	6	9 ^e	nr	Copperthwaite et al. ⁷⁹
Fe–Mn–K–C	330	15	2	98	30	43	21	Zhang et al. ⁸⁰
Fe–Ti–Mn–zeolite	450	10	0.5	10	25 ^d	49 ^d	nr	Sano et al. ⁸¹
MoO ₃ –Al ₂ O ₃ –K ₂ O	300	21	0.5	37	25	26	nr	Murchison et al. ⁸²
In ₂ O ₃ –CeO ₂	350	0.7	3	55 ^g	24 ^d	65 ^d	45	Arai et al. ⁸³
Mo ₂ C	300	0.03	1	nr	35 ^d	59 ^e	nr	Kojima et al. ⁸⁴
Mo ₂ C–K	297	1	3	70	nr	55 ^h	~50	Park et al. ⁸⁵
Co–Ce–SiO ₂	450	1	2	95	15 ^d	51 ^d	nr	Mirzaei et al. ⁸⁶
Co–Th	240	1	2	nr	34 ^c	32 ^d	nr	Costa et al. ⁸⁷
Zr–Al	400	17	nr	22	nr	67	nr	Yao et al. ⁸⁸

^aProduct selectivities are reported excluding CO₂. ^bSyngas conversion. ^cMole percent (%). ^dCarbon-based selectivity (% C). ^eC₂ + C₃. ^f% of alkenes in the C₂–C₄ fraction. ^gCO converted to hydrocarbons (%). ^hC₂–C₅ olefins.

and chemical promoters.⁵⁷ Table 2 shows that product selectivity toward short-chain hydrocarbons (C₁–C₆) and light olefins for the HTFT process is almost three times higher than for the low temperature process. The shift of product selectivity to short-chain hydrocarbons is reflected in the lower α and the 2-fold increase in methane selectivity.

Between the mid 1970s and mid 1980s Ruhrchemie A. G. developed different catalysts for the HTFT process by mixing iron oxide with oxides of other metals such as Ti, V, Mo, W, or Mn. It was reported by Büssemeier et al.^{58,59} that mixed oxide catalysts could produce lower olefins with a selectivity of 70% while exhibiting a low methane production (~10%) at CO conversions of about 50% (280 °C, 10 bar, H₂/CO = 1). They also reported that a catalyst prepared by sintering of Fe, Ti, Zn, and K oxides displayed high light olefins selectivity (75%) and low methane selectivity (10%) at high syngas conversion (87%) when tested at 340 °C.⁶⁰ The catalyst life in both cases was

mentioned to be some hundreds of hours. This type of catalyst exhibits extensive carbon deposition, and difficulties to reproduce the results have been encountered.⁵⁵

Roy et al.⁶¹ studied catalysts with similar composition as the fused catalysts patented by Ruhrchemie⁶⁰ but prepared by precipitation of iron nitrate in the presence of titania and further impregnation of the precipitate with Zn and K. The highest selectivity to light olefins they observed with the Fe–TiO₂–ZnO–K₂O catalyst was obtained at a syngas conversion of 45%, 250 °C, 2.5 bar, and H₂/CO = 1. The selectivity to C₂–C₃ olefins was 68%, and no C₄ products were reported while methane selectivity was approximately 20%.

Other mixed oxide catalysts were investigated by Goldwasser et al.⁶² who prepared perovskite-like oxides by doping a LaFeO₃ matrix with K and/or Mn to obtain La_{1-x}K_xFe_{1-y}Mn_yO₃ oxides. When these materials prepared by coprecipitation were tested at 280 °C, 11 bar, and H₂/CO = 2,

a high light olefins selectivity (70%) was observed in combination with a low methane production (10%) at low CO conversion (14%).

Although it has been reported that bulk mixed oxide catalysts are quite selective to lower olefins, they have not been applied in commercial processes, most probably due to their low stability.⁵⁵ Attempts to improve the stability of these systems included the modification of the catalysts by precipitating the oxides in the presence of a structural promoter such as SiO₂ or Al₂O₃;⁶³ however, for these modified catalysts the achieved lower olefins selectivity was low (<30% C). A summary of the different bulk catalysts proposed for the direct production of lower olefins from synthesis gas is presented in Table 3.

3.1.1. Alkali Metals and Sulfur as Promoters. It has been shown by many researchers that the addition of promoters can improve lower olefins selectivity of iron-based catalysts. The promoters that are most commonly used are alkali metals. Potassium has been extensively studied as a promoter for iron catalysts, and it has been reported that it increases the chain growth probability and enhances the production of olefinic hydrocarbons. Furthermore, it has been claimed that potassium has an effect on structural properties of bulk catalysts such as surface area and pore size^{89–93} and that its addition affects the extent of reduction and carbidization.^{94,95} Similar effects have been observed for sodium.^{92,96,97}

The effect of alkali promoters on product selectivity and catalytic activity is highly dependent on the concentration of the promoters, the preparation method, and the reaction conditions. Kang et al.⁶⁴ investigated the influence of the synthesis method on the performance of Fe–Cu–Al–K catalysts. They prepared two unsupported catalysts with similar compositions using the coprecipitation and sol–gel methods and two supported catalysts prepared by wet impregnation and impregnation/coprecipitation. The catalysts were tested at 300 °C, 10 bar, and H₂/CO of 2 for 70 h. The sample prepared with the sol–gel method exhibited the highest C₂–C₄ hydrocarbons selectivity (21%), with a yield of olefins of 11% and low methane selectivity (7%) at high CO conversion (96%). Kang et al. observed that C₂–C₄ selectivity and olefinic content decreased with an increase of surface acidity.

Bulk alkali-promoted catalysts have not only been prepared by coprecipitation or sol–gel methods but also by impregnation of preformed iron particles such as polycrystalline iron whiskers⁶⁵ or iron particles prepared from carbonyl precursors.⁶⁶ Hoffer et al.⁶⁶ reported a C₂–C₄ olefins selectivity of 44% with low methane selectivity (15%) at high CO conversion (98%) when Na-promoted Fe particles were tested at 340 °C, 23 bar, and H₂/CO of 1 (TOS = 60 h).

Although bulk catalysts promoted with Na or K have shown high selectivities to light olefins, their main disadvantage is that they suffer from fragmentation and attrition originated by the formation of carbon deposits or by phase transformations during carbide formation within large iron oxide crystals.^{67,68,98}

Sulfur has also been used as a chemical promoter to increase lower olefins selectivity. Sulfur is widely known as a very effective poison for Fischer–Tropsch catalysts, especially in the case of cobalt-based systems. However, some studies have shown that for Fe catalysts sulfur might act as a promoter, enhancing light olefins selectivity, reducing methane formation, and even increasing catalytic activity at low concentrations and under specific reaction conditions.^{69,99–101}

Crous et al.⁷⁰ filed a patent application for a catalyst with high selectivity to light olefins which consisted of a bulk iron

oxide promoted with an alkali metal and a second promoter of the group: Be, Ge, N, P, As, Sb, S, Se, and Te. They reported high selectivity to lower olefins (39%) and low methane formation (9%) with a syngas conversion of 41% when a precipitated catalyst promoted with sodium and sulfur was tested in the Fischer–Tropsch reaction at 330 °C, 20 bar, and a H₂/CO of 4.

Other studies have been performed with sulfur promoted catalysts where the promoter was not added during the preparation of the catalyst but it was incorporated in the catalytic system through exposure to H₂S.^{71,102} Hadadzadeh et al.⁷¹ investigated the effect of H₂S poisoning on catalysts prepared by coprecipitation of Fe and Mn nitrates in the presence of a structural promoter (titania, silica, alumina, magnesia, or zeolite). Their results showed that the sulfur-poisoned catalysts exhibited higher ethylene and propylene selectivities and lower methane production and activity when tested at 450 °C, 1 bar, and H₂/CO of 2. Hadadzadeh and co-workers focused their research on the influence of the different structural promoters and preparation conditions on activity and selectivity, but the effect of the promoters on stability was not specifically addressed.

3.1.2. Bimetallic Systems. Another strategy used by several researchers to improve the catalytic performance of catalysts for the direct production of lower olefins from synthesis gas is the use of Fe-based bimetallic catalysts. Among them, Co–Fe^{67,68,72–74} and Fe–Mn^{23,69,71,72,75–80,103} catalysts are the most studied systems. In the case of Co–Fe catalysts, the researchers intended to improve catalytic stability and activity of the already olefin-selective Fe catalysts by alloying it with a more active Fischer–Tropsch catalyst like Co. The bulk Co–Fe catalysts are generally prepared by coprecipitation, and they are usually promoted with chemical promoters such as K, Cu, and/or Mn and modified with structural promoters such as SiO₂ or Al₂O₃.

Tihay et al.^{67,68} reported on Co–Fe catalysts which contained both an alloy and a spinel phase. The catalysts were prepared by coprecipitation of iron and cobalt chloride solutions with KOH. The highest C₂–C₄ olefins selectivity was observed for a catalyst with a Co/Fe of 0.45. This sample was tested at 250 °C, 10 bar, and a H₂/CO of 1. At low CO conversion (~5%), a light olefin selectivity of 52% was obtained while methane production was high (34%). It was reported that this catalyst was stable for 200 h.

González-Cortés et al.⁷² studied Mn-promoted Co–Fe catalysts which were prepared as mechanical mixture of the metal oxides. The catalysts were tested at 300 °C, 1 bar, and a H₂/CO of 1. Under these conditions a catalyst with a molar composition of 100Fe:20Co:20Mn exhibited a C₂–C₄ olefins selectivity of 25% (CO conversion: 60%), which was the highest obtained for the studied Fe–Co–Mn systems. In comparison, an unpromoted Fe catalyst displayed a lower but stable CO conversion (40%) with a light olefins selectivity of ~32% and similar methane selectivity (~35%).

Fe–Co oxides prepared by coprecipitation of cobalt and iron nitrates in the presence of a structural promoter (1.5 wt % of TiO₂, SiO₂, Al₂O₃ or La₂O₃) were investigated by Mirzaei et al.⁷³ After optimization of preparation procedure, catalyst composition and reaction conditions, they reported that a potassium promoted (1.5 wt %) 40Fe:60Co (molar basis) catalyst modified with SiO₂ showed ~48% of ethylene and ~20% of propylene in its product composition when tested at 450 °C, 1 bar, and a H₂/CO of 4 (CO conversion ~85%). The

catalyst was found to be active and stable for 72 h under these reaction conditions, and selectivities to other products were not specified.

A recently published work from Feyzi et al.⁷⁴ on Fe–Co catalysts prepared by coprecipitation of Fe and Co nitrates using the water–oil microemulsion technique reported that a K-promoted (2 wt %) 75Co:25Fe (molar basis) catalyst tested at 260 °C, 1 bar, and H₂/CO of 2 exhibited a C₂–C₄ olefins selectivity of ~54% while maintaining a low methane production at high CO conversion (~64%). Increasing the operating pressure from 1 to 10 bar resulted in an increase of CO conversion (~73%) and in a further decrease in methane selectivity (~7%). However, it had a negative impact on light olefins selectivity that decreased to ~33%.

Even though it has been claimed that Mn is an effective promoter to decrease methane selectivity and to increase C₂–C₄ olefins selectivity of Fe-based catalysts, the results reported by different research groups vary depending on the preparation method, catalyst composition, pretreatment, and reaction conditions.

Van Dijk et al.⁶⁹ did not observe any effect of Mn on olefins selectivity when Fe–Mn catalysts were prepared by coprecipitation of Fe and Mn nitrates and when they were tested at 240 °C, 1 bar, and H₂/CO of 1 (CO conversions were kept below 5%). When reaction temperature was increased to 350 °C, the Fe–Mn catalysts produced mainly methane. The impregnation of an Fe–Mn catalyst with a solution of ammonium sulfate resulted in a 5-fold more active catalyst that produced olefins more selectively (CH₄, 28%; C₂H₆, 2%; C₂H₄, 45%). The sulfated (Fe_{at}/S_{at} = 200) and unsulfated catalysts exhibited a high extent of carbon deposition. Nevertheless, the sulfated catalysts displayed a lower mechanical strength evidenced by the disintegration of the catalyst particles after few hours. Van Dijk et al. indicated that higher quantities of S improved the resistance to carbon deposition, improving mechanical stability while maintaining a high C₂–C₄ olefins selectivity. The sulfur levels were maintained below 1 wt % to avoid catalyst deactivation via poisoning.

Soled et al.⁷⁷ prepared Fe–Mn catalysts as solid solutions by mixing Mn₃O₄, Fe₂O₃, and Fe powder and sintering the mixture at temperatures above 800 °C. The catalysts were promoted by impregnation of potassium carbonate or sulfate. When the catalysts were tested at 300 °C, 22 bar, and H₂/CO of 1, they exhibited a high CO conversion (>94%), low methane production, and high light olefins selectivity. The catalysts promoted with potassium sulfate displayed a C₂–C₆ olefins selectivity almost two times higher than the sample promoted with potassium carbonate (~34%) and a lower methane selectivity (~10%).

Manganese promoted Fe and Fe–Co catalysts were compared by González-Cortés et al.⁷² In comparison with unpromoted Fe catalysts, Fe–Mn samples displayed lower C₂–C₄ olefins selectivities (~26%) and higher methane production (~44%) when the reaction was carried out at 300 °C, 10 bar, and H₂/CO of 1. In general, the Fe–Mn catalysts modified with Co showed higher methane selectivities compared to the catalysts without Co.

Wang et al.²³ investigated Fe–Mn catalysts prepared by the sol–gel method or by coprecipitation. Both types of catalysts were tested at 350 °C, 15 bar, and a H₂/CO of 2 (TOS = 300 h). The highest light olefins selectivity was achieved with a coprecipitated catalysts (15:85 Mn:Fe). At a very high CO conversion (>90%), this catalyst showed a high C₂–C₄ olefins

selectivity (~50%) and a methane selectivity of about 30%. They attributed the higher yield of alkenes obtained with coprecipitated catalysts to better carbidization and reduction properties. The results obtained by Wang et al. pointed out that catalyst preparation is a key aspect that can determine the performance during reaction.

Zhang et al.⁸⁰ added carbon as a structural modifier for their Fe–Mn–K catalysts prepared via the sol–gel method. The catalysts were tested at 330 °C, 15 bar, and H₂/CO of 2. The highest C₂–C₄ olefins selectivity (~43%) was achieved at a high CO conversion (~98%) along with a methane selectivity of about 30%. The chain growth probability (α) decreased with an increase of the content of structural modifier while the C₂–C₄ fraction increased achieving a maximum at 5 wt % carbon content. Zhang and co-workers claimed that carbon promoted the formation of nanoparticles, which enhanced the selectivity to light olefins.

Other bimetallic iron-based systems have been studied such as the coprecipitated Ni–Fe catalysts modified with alumina.¹⁰⁴ Nickel is a well-known methanation catalyst, and it is expected that it would have a negative influence on the alkene to alkane ratio due to its high activity for hydrogenation. The research study by Cooper et al.¹⁰⁴ showed that the addition of Ni to bulk Fe catalysts results in a low alkene/alkane ratio when the Ni content was below 60%. Contrary to what was expected, bulk Ni–Fe catalysts with 60 or 80 wt % of Ni exhibited an alkene/alkane ratio of approximately 4 or 2, respectively.

A graphical summary of the bulk catalysts with the highest selectivity to lower olefins is displayed in Figure 9.

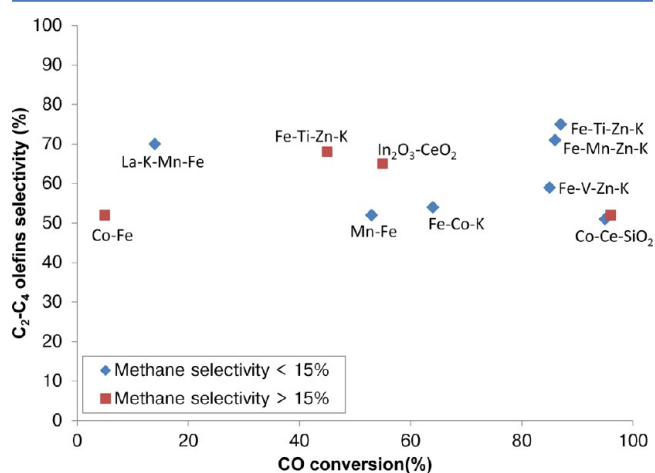


Figure 9. Bulk catalysts for the FTO reaction (C₂–C₄ olefins selectivity >50%). Catalysts with CH₄ selectivities below 15%: diamonds.

From Figure 9 it can be observed that selectivities to C₂–C₄ olefins up to 75% were obtained using potassium-promoted catalyst. These catalysts were synthesized combining different promoters. The results reported for the Fe–Ti–Zn–K and Fe–Mn–Zn–K catalysts indicated that these catalysts not only had a high selectivity to lower olefins and low methane production but also a high activity (CO conversion ~90%). However, these results have been difficult to reproduce^{55,69} probably originated by the complex structure of the catalyst, the presence of impurities in the precursors, or differences in the activation procedure.

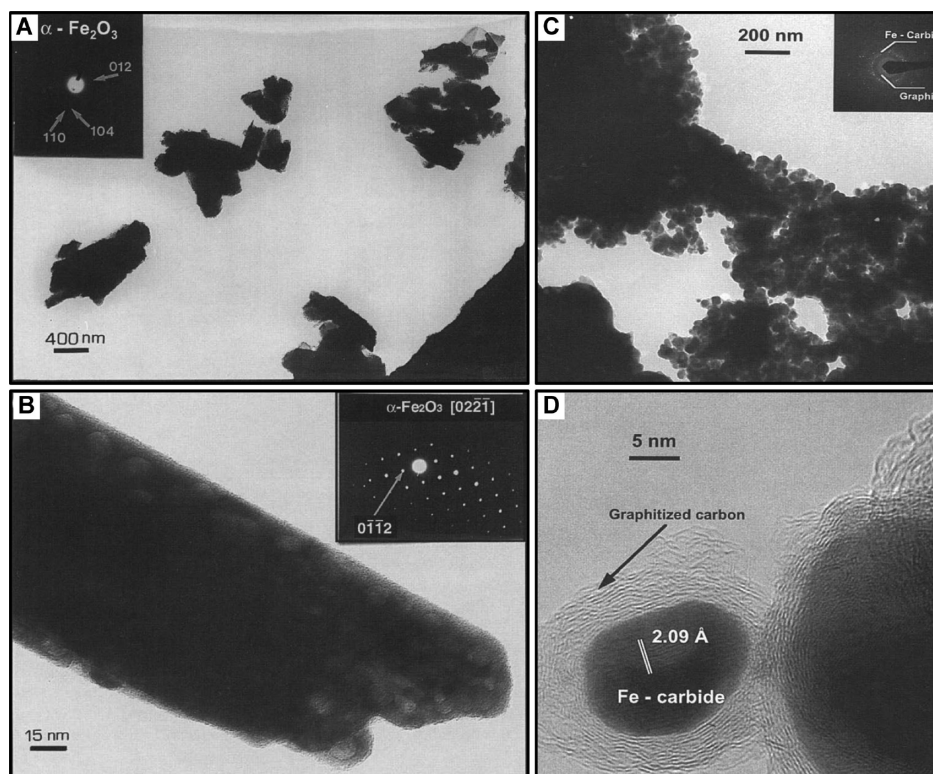


Figure 10. Fragmentation of bulk Fe catalysts upon exposure to CO. A, B: TEM images of a bulk iron catalyst before reaction. Electron diffraction showed that the primary particles were single α -Fe₂O₃ crystals. C, D: Micrographs after the catalyst was put in contact with CO at 400 °C. The individual particles were identified as iron carbide and were covered by graphitic carbon. Adapted with permission from Kalakkad et al.⁹⁸ Copyright 1995 Elsevier.

3.1.3. Non-Fe-Based Catalysts. Research studies have been performed as well on catalytic systems that do not contain Fe (carbide) as an active phase for the production of light olefins from synthesis gas. These non-Fe-based catalysts vary in composition from Co¹⁰⁵ and precipitated K₂MoO₄⁸² to multicomponent systems such as Co–Mn.⁷⁹ Other non-Fe-based catalysts have been used for the selective production of ethylene such as coprecipitated Cu–Cr–Co–Al₂O₃¹⁰⁶ or for the preferential synthesis of ethylene and propylene using coprecipitated In₂O₃–CeO₂⁸³ or Mo₂C.⁸⁴

Potassium promoted molybdenum catalysts were developed by Park et al.⁸⁵ These catalysts showed C₂–C₅ olefins selectivities up to 60% at high CO conversion (70%) when they were tested under the Fischer–Tropsch reaction at 297 °C, 1 bar, and H₂/CO = 3.

Cobalt based systems have been investigated by different research groups.^{86,87,107} Mirzaei et al. studied the effect of catalyst preparation conditions (Co/metal ratios, aging time, and calcination temperature), structural promoters (titania, silica, alumina, or zeolite), and reaction conditions (H₂/CO and reaction temperature) on catalytic performance. A Co–Ce catalyst modified with SiO₂ and tested at 450 °C, 1 bar, and H₂/CO of 2 exhibited a high C₂–C₄ olefins selectivity (~50%) with low methane production (15%) at a CO conversion of 90%.⁵³ Mirzaei et al.¹⁰⁷ also reported on a Co–Mn–TiO₂ catalyst with high selectivity to ethylene and propylene (~15% and ~85%, respectively) at a CO conversion of 65%. Selectivities toward other products were not reported. Their results were obtained at 450 °C, 1 bar, and H₂/CO = 3.

Costa et al.⁸⁷ reported on a catalyst prepared by mixing dicobalt octacarbonyl and thorium acetylacetonate in a

hydrogenated terphenyl. The solution was heated up at 200 °C to decompose the metal precursors forming a slurry catalyst. Syngas with a H₂/CO ratio of 2 was introduced in the catalyst suspension, and the reaction was carried out at 240 °C and 1 bar. It was reported that 88% of the hydrocarbons formed corresponded to the C₁–C₅ fraction with an olefin content of more than 80%.

A high selectivity to lower olefins was observed by Yao et al.⁸⁸ when they performed the Fischer–Tropsch reaction at 400 °C and 18 bar using a Zr–Al catalyst. They reported a C₂–C₄ olefins selectivity of 67% at a CO conversion of 22%. The H₂/CO ratio used for the reaction and the selectivity to methane and other hydrocarbons were not specified.

Promoted bulk catalysts could be considered as the most interesting option for FTO because of their high selectivity to light olefins, low methane production, low cost, and simple synthesis procedures. However, it is known that unsupported iron catalysts that are used for the Fischer–Tropsch reaction at high temperatures (>300 °C) and CO-rich syngas suffer from low mechanical stability. Bulk Fe catalysts tend to fragment due to carbon deposition or to density differences between the oxidic and carbidic phases present in the working catalyst.^{98,108} In the case of carbon deposition it has been shown that bulk Fe catalyst particles break up and formation of fines may pose problems.^{109,110} By moving to supported catalysts the carbon is to a certain degree contained in the pores, iron particles are much smaller, and fragmentation is delayed or does not occur.

Figure 10 illustrates the structural changes of bulk iron catalysts upon carbidization. The large Fe₂O₃ crystals fragmented upon contact with CO at high temperature due to stress originated inside the particle by the formation of the

carbide phase or by nucleation of carbon deposits (Figure 10C). The formation of iron carbide is necessary for the Fischer–Tropsch reaction as it is recognized as the active phase.^{108,111} Advances in characterization techniques have allowed the investigation of carbide formation in working bulk Fe catalysts under industrially relevant conditions.^{112,113}

In Figure 10D it is clearly observed that the small carbide particles were covered with a layer of graphitic carbon. In some cases, the carbon deposits grow as fibrils or filaments as observed by Torres Galvis et al.⁵⁵

A strategy to avoid or to restrict the nucleation of carbon deposits on iron-containing particles is to reduce their size from micrometers to nanometers. Small iron nanoparticles do not fragment further when they are put in contact with syngas at high temperatures; however, if they are close together, they tend to aggregate, forming large particles, which ultimately nucleate carbon and fragment.¹¹⁴ The use of a support material increases the stability of iron-based catalysts by serving as a mechanical anchor that maintains the nanoparticles separated, avoiding the formation of clusters and particle growth. Several supports have been proposed for the dispersion of the active phase of FTO catalysts ranging from oxides and molecular sieves to clays and carbonaceous materials. The supported catalysts that have been used to selectively produce light olefins from synthesis gas are discussed in section 3.2.

3.2. Supported Fe Catalysts. Support materials are used in the preparation of heterogeneous catalysts to maximize the surface area of the active phase. For this reason, carrier materials with large surface areas such as silica or gamma alumina are traditionally preferred. Catalysts containing highly dispersed iron nanoparticles can be easily prepared by impregnating conventional high surface area supports with inorganic iron salts. The iron-containing nanoparticles of these catalysts have a relatively narrow size distribution and a homogeneous spatial distribution thus minimizing the formation of aggregates. Nevertheless, iron has a strong interaction with most of the oxidic supports, which results in the formation of mixed iron oxides that are not active for the Fischer–Tropsch reaction. It is known that iron aluminates^{115,116} and iron silicates^{117–119} are difficult to reduce, which hinders the formation of the carbidic active phase. Consequently, catalysts prepared on γ -alumina or silica exhibit lower activities compared with catalysts supported on inert carriers.⁵⁵ Although a weakly interactive support allows activating the iron phase and facilitates a close contact between iron and chemical promoters, the weak physical binding between its surface and iron nanoparticles does not withstand the reaction conditions. As a result, iron-containing nanoparticles aggregate extensively and the catalyst deactivates due to a reduction in the active surface and to increased coke lay-down.¹¹⁴ A schematic representation of the improved stability achieved when using a support material is shown in Figure 11.

In view of the importance of the nature of the support and its influence on catalytic performance extensive research has been performed to find an optimal combination of active metal, support, and modifiers. In the following sections, we will discuss the different catalysts that have been used for the synthesis of lower olefins via Fischer–Tropsch. The catalytic performance of these materials is summarized in Table 4.

3.2.1. Silica Supported Catalysts. Bruce et al.¹²⁰ prepared Fe, Fe/Mn, Fe/K, and Fe/Mn/K catalysts by impregnation of silica gel with metal nitrates. For a comparison, they synthesized also Fe/Mn/K and Fe/Mn supported catalyst

Supported Catalyst

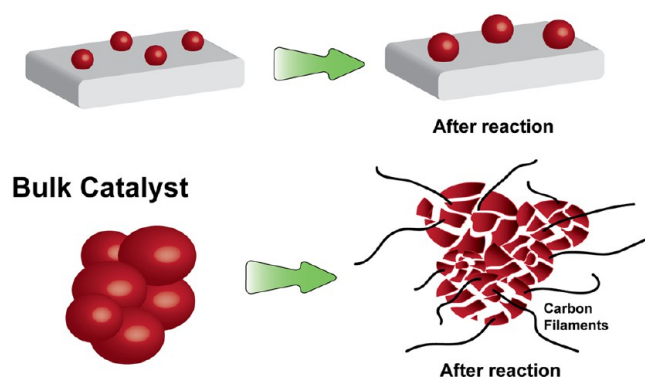


Figure 11. Stabilization of iron-containing nanoparticles using a support.

using Fe/Mn or Fe/Mn/K carbonyls. The catalysts were tested at 300 °C, 2–5 bar, and a H₂/CO ratio of 1.5. Under low CO conversion (<5%), a high selectivity toward lower olefins (64%) and low methane production (25%) was observed for the Fe/Mn/K carbonyl-based catalyst. Bruce and co-workers attributed the higher light olefin selectivity of the carbonyl-derived catalysts to a minimization of secondary hydrogenation reactions. It is expected that the impregnation of organometallic complexes would lead to better iron dispersions in comparison with iron nitrate which rapidly crystallize upon drying.¹⁵⁵ However, morphological or chemical differences between nitrate-based and carbonyl-based were not specifically mentioned.

A similar approach was used by Commereuc et al.¹²¹ who prepared supported iron catalyst using iron carbonyl precursors and different oxidic supports. A high olefin selectivity (69%) was achieved when using an Fe/SiO₂ catalyst synthesized by impregnation of iron pentacarbonyl. The reaction conditions were 265 °C, 10 bar, H₂/CO of 1, and low CO conversion (5%).

Stoop et al.¹²² reported a high olefin selectivity when performing the Fischer–Tropsch reaction with a Ru/Fe (1:3) silica supported catalyst at 277 °C, 1 bar, and H₂/CO of 2. At CO conversions below 3%, this bimetallic catalyst exhibited low methane selectivity (10%) and high olefin to paraffin ratios (ethylene/ethane, 3; propylene/propane, 16). The Ru/Fe alloy combined the high olefin selectivity of Fe with the high catalytic activity of Ru. Interestingly, thermogravimetric studies showed that carbon deposition rates of the Ru/Fe (1:3) catalyst were higher than for unpromoted Fe/SiO₂. When reaction temperature was increased to 402 °C, the amount of carbon deposited increased steeply with time, causing severe deactivation.

Another bimetallic system was studied by Cooper et al.,¹⁰⁴ who investigated Fe/Ni catalysts supported on silica. In contrast with the bulk Fe/Ni catalysts discussed in section 3.1.2, the Fe–Ni/SiO₂ catalysts with Ni contents higher than 60% showed low alkene to alkane ratios. At lower Ni loadings, the effect of Ni on olefins selectivity was negligible.

A different approach to improve the light olefins selectivity of Fe/SiO₂ catalysts was proposed by Jiang et al.,¹²³ who combined a Fischer–Tropsch active core with a zeolite shell to limit the formation of long hydrocarbons. The Fe/SiO₂ core was prepared by incipient wetness impregnation of iron nitrate, and the silicalite-1 shell was synthesized using a secondary growth method. When the composite catalyst was tested at 380

Table 4. Supported Catalyst for the Fischer–Tropsch to Olefins Process^a

catalyst: elements present	T (°C)	P (bar)	H ₂ /CO (molar)	CO convn (%)	CH ₄ (% wt)	C ₂ –C ₄ olefins (% wt)	CO convn to CO ₂ (%)	ref
Fe–Mn–K/SiO ₂	300	2–5	1.5	<5	25	64	nr ^b	Bruce et al. ¹²⁰
Fe/SiO ₂	265	10	1	5	21 ^c	69 ^{c,d}	nr	Commereuc et al. ¹²¹
Ru–Fe/SiO ₂	277	1	2	<3	26 ^c	60 ^{c,e}	nr	Stoop et al. ¹²²
Fe/SiO ₂ , sil-1 shell	380	10	0.5	21	21	30	nr	Jiang et al. ¹²³
Fe–Ce/heat treated γ -Al ₂ O ₃	280	8	0.5	3 ^f	8	58	nr	Baker et al. ¹²⁴
Fe–Pr/heat treated γ -Al ₂ O ₃	280	8	0.5	15 ^f	7	63	nr	Baker et al. ¹²⁵
Fe/Al ₂ O ₃	290	9	0.9	5	25	49	nr	Basset et al. ¹²⁶
Fe/ γ -Al ₂ O ₃	500	15	1	18	38	43	nr	Barrault et al. ¹²⁷
Fe–K/Al ₂ O ₃	260	1	3	1	23 ^g	60 ^g	nr	Arakawa et al. ¹²⁸
Fe/Al ₂ O ₃	470	15	1	20	29	41	nr	Barrault et al. ¹²⁹
Fe–Mn/Al ₂ O ₃	340	15	1	70	19 ^c	18 ^c	nr	Barrault et al. ¹³⁰
Fe–S/Al ₂ O ₃	470	15	1	14	28 ^c	42 ^c	nr	Barrault et al. ¹³⁰
Fe–Mn–S/Al ₂ O ₃	470	15	1	12	28 ^c	34 ^c	nr	Barrault et al. ¹³⁰
Fe–Na–S/ α -Al ₂ O ₃	340	20	1	80	11 ^c	53 ^c	~50	Torres Galvis et al. ⁵⁵
Fe–K/silicalite	280	21	0.9	nr	9	36	nr	Rao et al. ¹³¹
Fe–Cu–K/Zr-ferrierite	300	10	0.5	96	34 ^c	12 ^{c,h}	38	Bae et al. ¹³²
Fe–Cu–K/ZSM-5	300	10	2	81	20 ^c	30 ^c	36	Kang et al. ¹³³
Fe–Mn–K/silicalite-2	347	20	2	90	22	70	nr	Xu et al. ¹³⁴
Fe–Mn/silicalite-1	275	21	1	10	9	65	3	Das et al. ¹³⁵
Fe–Cu–K/ZSM-5	300	10	2	81	18	10	38	Kang et al. ¹³⁶
Fe/K-ZSM-5	300	14	1	9	10	37 ⁱ	nr	Mitsudo et al. ¹³⁷
Fe–Pd/ZnO	300	7	1	<10	45 ^g	30 ^g	nr	Gustafson et al. ¹³⁸
Fe–Mn/MgO	320	20	2	79	23	68	nr	Xu et al. ¹³⁹
Fe/MgO	176	1	0.5	1	26	58	nr	Hugues et al. ¹⁴⁰
Fe/MnO	270	1	1	10	12	59	28	Barrault et al. ¹⁴¹
Fe–Al-laponite	412	1	3	nr	28 ^c	43 ^c	20	Barrault et al. ¹⁴²
Fe/O-CNT	340	25	1	50	8	92 ^j	24	Schulte et al. ¹⁴³
Fe–Mn/C	250	1	1	nr	11	53	28	Barrault et al. ¹⁴⁴
FeN–Mn/CNT	300	5	1	12	24	44	36	Yang et al. ¹⁴⁵
Fe–Na–S/CNF	340	20	1	88	13 ^c	52 ^c	~50	Torres Galvis et al. ⁵⁵
Fe/activated carbon	350	1	1	2	18	61 ⁱ	nr	Sommen et al. ¹⁴⁶
Fe/C	230	1	3	3	40 ^g	32 ^{j,g}	nr	Jung et al. ¹⁴⁷
K[MnFe(CO) ₉]/C	290	1	3	1 ^e	25 ^g	76 ^g	nr	Venter et al. ⁸⁹
Co–Mn/SiO ₂	280	1	1	9	19 ^c	22 ^c	nr	Barrault et al. ¹³⁰
Co–Zn/TiO ₂	240	1	2	65	9 ^c	47 ^c	2	Feyzi et al. ¹⁴⁸
Co/silicalite-1	275	21	3	49	27	33	12	Das et al. ¹⁴⁹
Mo–K/ZrO ₂	300	21	1	92	19 ^c	65 ^{c,h}	nr	Murchison et al. ⁸²
Ru/TiO ₂	k	1	1	1	26	47	nr	Vannice et al. ¹⁵⁰
Ru–Na/TiO ₂	270	0.5	2	nr	18 ^c	68 ^c	25	Doi et al. ¹⁵¹
Ru/Al ₂ O ₃	200	0.7	2	10–25	8	70	2	Okuhara et al. ¹⁵²
Ru/CeO ₂	354	21	1	10	16	39	nr	Pierantozzi et al. ¹⁵³
Ru/V ₂ O ₃	243	1	3	4	45 ^g	28 ^g	nr	Vannice et al. ¹⁵⁴

^aProduct selectivities are reported excluding CO₂. ^bNot reported. ^cCarbon-based selectivity (% C). ^d% olefins in hydrocarbons. ^eC₂–C₅. ^fCO converted to hydrocarbons (%). ^gMole percent (%). ^h% of alkenes in the C₂–C₄ fraction. ⁱC₂ + C₃. ^j% of alkenes in the C₂–C₆ fraction. ^k262 – 274 °C.

°C, 10 bar, and H₂/CO of 2, it exhibited a light olefins selectivity of 30%, a CH₄ selectivity of 21%, and a CO conversion of 21%. In contrast, under the same reaction conditions the bare Fe/SiO₂ catalyst displayed a lower C₂–C₄ olefins selectivity (20%) but its CO conversion was almost double. The lower catalytic activity of the core–shell catalyst was tentatively attributed to limitations in the diffusion of the reactants and to possible effects on the iron phase by the hydrothermal zeolite synthesis.

Yeh and co-workers¹⁵⁶ studied the catalytic performance of silica supported iron carbides and iron nitrides. The highest selectivity to olefins (~25%) was observed for an Fe–K-

nitride/SiO₂ at low CO conversion (~1%), when it was tested under the Fischer–Tropsch reaction at 250 °C, 8 bar, and a H₂/CO ratio of 1.

3.2.2. Alumina Supported Catalysts. Baker et al.^{124,125} prepared iron oxide catalysts using heat-treated gamma alumina modified by impregnation of rare earth oxides. A high C₂–C₄ olefins selectivity (63%) and low methane production (7%) were observed when using an Fe–Pr/heat-treated γ -alumina at 280 °C, 8 bar, and H₂/CO ratio of 0.5. The highest yield of alkenes was achieved at low H₂/CO ratios (<1). Under these conditions iron-based catalysts exhibit extensive coke lay-

down;^{146,157} however, the researchers claimed that the catalyst had a long active life.

Organometallic compounds have been used not only for the preparation of Fe/SiO₂ but also for the synthesis of alumina supported catalysts. Basset et al.¹²⁶ filed a patent application on catalysts prepared by deposition of organometallic aggregates of Fe and/or Co and/or Ni on inorganic supports. The highest light olefins selectivity was obtained with a catalyst prepared with the precursor Fe₄(CO)₁₃H₂ which was impregnated on alumina (presumably alpha alumina, surface area 10 m²/g). The catalyst displayed a lower olefins selectivity of 49% and CH₄ selectivity of 25% at low CO conversion (5%) when used in the Fischer–Tropsch reaction at 9 bar, 290 °C, and H₂/CO of 0.9.

As previously mentioned, Commereuc et al.¹²¹ prepared different iron-based catalyst by impregnation of silica, lanthanum oxide, magnesium oxide, and alumina with Fe(CO)₅ or Fe₃(CO)₁₂ diluted in *n*-pentane. Most of the catalysts showed C₂–C₅ olefins selectivity higher than 40% when the reaction was carried out for 90 h at 10 bar and H₂/CO of 1. γ -Alumina supported catalysts prepared using different precursors, Fe(CO)₅ or Fe nitrate, displayed different catalytic performance. The catalyst prepared with iron nitrate exhibited a lower olefin selectivity (38%) compared with the sample prepared with iron carbonyl (57%). Commereuc and co-workers attributed the higher light olefins selectivity to a higher dispersion of iron-containing particles. The fresh carbonyl-based catalyst contained 2 nm Fe particles that sintered to form 20–50 nm particles after 90 h of reaction. Fe nanoparticle growth coincided with a decrease in olefins selectivity.

The influence of different alumina supports on catalytic activity was investigated by Barrault et al.¹²⁷ The catalysts were synthesized by precipitation of iron nitrate with ammonia in the presence of the carrier material. The reaction was performed at 15 bar and H₂/CO of 1, and the reaction temperature was varied from 280 to 500 °C according to the catalyst activity. The highest selectivity to light olefins (43%) was observed for a γ -alumina supported catalyst (400 m²/g). This catalyst showed a low activity at 280 °C, and it was necessary to increase reaction temperature to 500 °C to achieve a similar level of CO conversion (20%) than for catalysts prepared with aluminas with lower surface areas. Under these reaction conditions, the catalyst with the highest C₂–C₄ olefins selectivity displayed the highest methane selectivity (38%). The comparison of the catalytic properties of alumina supported catalysts showed that the most active catalysts were the least selective.

A Na- and S-promoted/ α -alumina catalyst with a high selectivity to light olefins was designed by Torres Galvis et al.⁵⁵ A homogeneous distribution of iron-containing nanoparticles is difficult to achieve in supports with low interaction toward iron such as α -alumina with a low surface area (~10 m²/g). Fe/ α -alumina catalysts prepared by impregnation of aqueous solutions of iron nitrate exhibit a poor distribution of iron nanoparticles.¹¹⁴ To achieve a more homogeneous spatial distribution of the particles, the researchers used ammonium iron citrate, a chelated iron complex, as a precursor. The catalysts were tested at 340 °C, 20 bar, and H₂/CO of 1. A high selectivity to light olefins (53%) and a low methane selectivity (11%) were achieved by introducing Na and S as chemical promoters.⁵⁶ The catalysts supported on inert carriers showed a higher activity in comparison with samples prepared with high surface area supports such as γ -alumina and silica. After 64 h of reaction, Na–S–Fe/ α -alumina displayed a stable catalytic activity, limited sintering, and relatively low coke lay-down

(<10%). In a further study, Koeken et al.¹⁵⁷ investigated the influence of process conditions on catalytic performance and the deactivation of Na–S–Fe/ α -alumina catalysts. Koeken and co-workers showed that the formation of carbon deposits can be suppressed for these catalysts by using higher H₂/CO ratios without affecting the catalyst selectivity.

3.2.3. Zeolite Supported Catalysts. Many research groups have explored the use of zeolites^{22,81,131–137,139} and aluminophosphate molecular sieves¹⁵⁸ as supports for iron-based FTO catalysts.

Rao et al.¹³¹ filed a patent application on an Fe–K/silicalite catalyst prepared by impregnation of K and Fe nitrates. The catalyst was tested at 280 °C, 21 bar, and a H₂/CO ratio of 0.9, and under these conditions a light olefins selectivity of 36% was obtained with a methane production of 9%. An Fe–Cu–K/zeolite catalyst developed by Bae et al.¹³² was prepared using a proton type ferrierite zeolite impregnated with a solution containing Fe and Cu nitrates and K carbonate. The reaction was carried out at 350 °C, 9.8 bar, and a H₂/CO of 2. The catalyst exhibited a C₂–C₄ hydrocarbons selectivity of 40% with a C₂–C₄ olefins yield of 12%. These promoted catalysts displayed higher light hydrocarbons and C₂–C₄ olefins selectivity compared with iron-based catalyst which did not contain zeolites. Additionally, it was claimed that the catalysts showed a limited deactivation with time on stream.

The design strategy used by Kang et al.¹³³ for a zeolite supported FTO catalyst was to use a bifunctional catalyst where the FT active metal transformed syngas into a primary straight hydrocarbon chain that underwent cracking on the acid zeolite to produce hydrocarbons of limited chain length. For the preparation Kang and co-workers used aqueous solutions or iron and copper nitrates and potassium carbonate to impregnate ZSM-5, mordenite, and beta-zeolite. The catalysts were tested at 300 °C, 10 bar, and a H₂/CO ratio of 2. Fe–Cu–K/ZSM-5, which had the lowest amount of acidic sites, showed a light olefins selectivity of 30% and CH₄ selectivity of 20% at a high CO conversion (81%). The structure of the mordenite and beta-zeolite supported catalyst was damaged during reaction.

Xu et al.¹³⁴ studied the promotion effects of K₂O and MnO on Fe/silicalite-2 for the selective production of light alkenes via syngas. The catalysts were prepared by impregnation and were tested at 20 bar, 347 °C, and a H₂/CO of 2. The highest C₂–C₄ olefins selectivity (70%) was obtained with a K–Fe–Mn catalyst (8.3%–9.5%–9.6%). They concluded that MnO restricted the hydrogenation of C₂H₄ and C₃H₆. They proposed that the addition of K₂O affected the CO adsorption, resulting in a higher CO conversion and a higher alkene selectivity. The researchers also put forward that K₂O inhibited the disproportionation and hydrogenation of C₂H₄.

Liu et al.²² performed experiments for direct syngas conversion over K–Fe–Mn/Si-2 catalysts at semipilot scale with the catalysts previously reported by Xu.^{134,139} The semipilot plant test was performed at 300–350 °C, 20 bar, and a H₂/CO ratio of 2. CO conversions between 70 and 90% were achieved with a light olefins selectivity between 71 and 74%. Despite the low hydrothermal stability that could be expected for zeolite supported catalysts, Liu and co-workers reported that the catalyst was stable for at least 1000 h. The K–Fe–Mn/Si-2 was regenerated after 1000 h, and it displayed nearly the same properties as the fresh catalyst. From the comparison of the bench scale tests performed made by Liu et al., they concluded that the direct method had a lower light

olefin yield compared with the synthesis of lower olefins via dimethyl ether.

Das et al.¹³⁵ reported on the effect of Mn addition to silicalite-1 supported Fe and Co catalysts. The catalysts were prepared by impregnation of silicalite-1 with Fe, Co, or Mn nitrate solutions. The samples were tested at 275 °C, 21 bar, and H₂/CO of 1. A high selectivity to lower olefins (65%) was reported for an Fe–Mn/Sil-1 catalyst (10% Fe, 5% Mn) at a low CO conversion (5%). The researchers concluded that Mn reduced iron oxide particle size and hindered carburization. They attributed the increased olefin selectivity to the presence of Fe³⁺ in the catalyst.

The effect of the Si/Al ratio of ZSM supported catalysts on catalytic performance was studied by Kang et al.¹³⁶ They synthesized the catalysts by impregnation of proton ZSM-5 with different Si/Al using Fe and Cu nitrates and potassium carbonate. The catalysts were tested at 300 °C, 10 bar, and H₂/CO of 2 for 70 h. An Fe–Cu–K/zeolite with a low Si/Al ratio (Si/Al = 25) showed the highest CO conversion (81%) and the highest C₂–C₄ olefins (10%).

3.2.4. Other Oxidic Supports. Gustafson et al.¹³⁸ filed a patent application on palladium-promoted Fe catalysts supported on ZnO. The catalysts were prepared by impregnation of Pd and Fe nitrates. A moderate light olefin selectivity (30%) and a high methane production (45%) were achieved when the samples were tested at 300 °C, 7 bar, and a H₂/CO ratio of 1.

Xu and co-workers¹³⁹ prepared Fe–Mn catalysts by impregnation of silica, alumina, ZrO₂, TiO₂, and MgO. The researchers highlighted the importance of the selection of the support material since its properties, e.g., acid-basic properties, metal–support interaction, structures of channels and micropores, have a major impact on catalytic performance. They reported that Fe–Mn catalysts synthesized on a basic supports could produce up to 70% of light olefins while maintaining a high activity (70–90% CO conversion) under certain reaction conditions. The highest light olefins selectivity (68%) was achieved using an Fe–Mn/MgO catalyst at 320 °C, 20 bar, and H₂/CO ratio of 2. Xu et al. ascribed the high olefins selectivity of Fe–Mn/MgO catalysts to a stronger CO adsorption originated by the basicity of the support.

Magnesium oxide was also used by Hugues et al.¹⁴⁰ for the preparation of catalysts for the selective formation of propene from syngas using Fe₃(CO)₁₂ as metal precursor. A high C₂–C₄ olefins selectivity was observed (58%) when testing the Fe/MgO catalyst at 176 °C, 1 bar, and a H₂/CO ratio of 0.5.

Barrault et al.¹⁴¹ studied the production of lower olefins from syngas using manganese oxide supported catalysts. The catalysts were prepared by impregnation of MnO or MnO₂ with iron nitrate, Fe(Acac)₃, or Fe(Acac)₂. A high selectivity to light olefins (59%) was obtained when using an Fe(C₃H₇O₂)₃/MnO₂ catalyst tested at 350 °C, 1 bar, and a H₂/CO ratio of 1. Their results demonstrated that an adequate Fe/Mn stoichiometry is needed for selective conversion of syngas into light olefins and that the nature of iron precursor and the preparation method have a large impact on catalytic activity and selectivity. Barrault and co-workers¹⁴² also explored the use of ion-exchanged pillared laponites for the Fischer–Tropsch synthesis of lower olefins from synthesis gas.

3.2.5. Carbon Supported Catalysts. Carbonaceous materials are an interesting alternative for the preparation of supported catalysts. Carbon supports can be obtained with surface areas ranging from 150 to 1500 m²/g, with diverse pore sizes and

pore structures, and their surface can be modified to tune their affinity with metal precursors.^{49,159,160} Carbon supports are relatively inert, and they can display a weak interaction with iron depending on their surface properties.

Activated,^{89,90,144,146,161} graphitic, and glassy carbons¹⁴⁷ have been used by several research groups to synthesize supported Fe catalysts for the production of lower olefins from syngas. Venter et al.⁸⁹ prepared Fe/C catalysts using amorphous carbon black as support and impregnating with organometallic mixed-metal carbonyl clusters (Mn, Fe, and/or K). The catalysts were tested at 275–290 °C, 1 bar, and a H₂/CO ratio of 3. Under these reaction conditions, a K[MnFe(CO)₉]/C catalyst displayed a light olefins selectivity of 76% while no paraffins were detected. It is important to note that the researchers reported that their carbon support contained sulfur. The presence of sulfur in low concentrations could have improved the catalysts' selectivity toward lower olefins as previously discussed in section 3.1.1. Venter et al. reported that better catalytic performances could be achieved using carbonyl precursors instead of metal nitrates. They also mentioned that the pretreatment method has a strong influence on selectivity and activity.

In a further study, Venter and co-workers⁹⁰ reported on the stability of their catalytic systems. The catalysts stabilized within 24 h, and the high olefin to paraffin ratio remained unchanged during long periods on stream. Activity declined about 55% compared to the initial value after 100 h, and the deactivation was mainly due to carbon deposition and not to sintering. The high stabilities of the K–Mn–Fe/C catalysts were related to the high H₂/CO ratio used during reaction. The researchers claimed that these catalysts could be regenerated with reduction under H₂ at 350 °C for 16 h.

Barrault et al.¹⁴⁴ filed a patent application on an Fe–Mn/AC catalyst prepared using acetyl-acetonate complexes. They reported a C₂–C₄ olefins selectivity of approximately 50% when the catalyst was tested at 250 °C, 1 bar, and a H₂/CO of 1.

Activated carbons have very high surface areas, and they are relatively cheap, as they are generally produced by carbonization of nutshells, wood, and other natural carbon sources. However, they usually contain traces of other elements that might act as promoters or poisons for the Fischer–Tropsch active metals. Carbon materials with more controlled morphologies and higher purities can be synthesized in the form of carbon nanotubes (CNTs) or carbon nanofibers (CNFs).

Yang et al.¹⁴⁵ investigated the effect of Mn and K on the catalytic performance of FeN catalysts confined in CNTs. Yang and co-workers synthesized the FeN catalysts by introducing an iron nitrate solution into the CNT channels using ultrasonication and stirring. The nitridation process was performed using ammonia. The promoted samples were prepared using a solution containing Fe, Mn, and K nitrates. The catalysts were tested at 300 °C, 5 bar, and a H₂/CO ratio of 1. The addition of Mn reduced CO conversion to 12% and increased light olefins selectivity to 44%. The researchers stated that addition of K did not affect activity or selectivity under the studied reaction conditions.

Schulte et al.¹⁴³ used CNT as support to prepare supported iron catalysts. They studied the influence of CNT surface modification on catalytic performance. Oxygen- and nitrogen-functionalized CNTs were impregnated with ammonium iron citrate and tested at 340 °C, 25 bar, and a H₂/CO of 1. The

highest light olefins selectivity (up to 92% of alkenes in the C₂–C₆ fraction) was obtained with an Fe/O-CNT which also exhibited a low methane selectivity (9%) at a CO conversion of 45%. The catalysts reported in this study exhibited a high and constant CO conversion for a period of 80 h time on stream. The catalysts supported on nitrogen-functionalized CNT's showed a slower deactivation compared with O-CNTs.

Surface-oxidized carbon nanofibers were used by Torres Galvis et al. to prepare Na–S-promoted iron catalysts.⁵⁵ The CNF supported catalyst showed a high selectivity to C₂–C₄ olefins (52%) at high CO conversion (88%) when the FTO reaction was performed at 340 °C, 20 bar, and a H₂/CO ratio of 1. The catalyst showed a stable activity during 64 h of reaction. In a complementary study, Torres Galvis et al. investigated the influence of iron (carbide) particle size on catalytic performance using CNF supported catalysts.¹⁶² The researchers concluded that the surface-specific catalytic activity increases with decreasing iron particle size, which is, surprisingly, in contrast to results found for Co nanoparticles on carbon nanofibers.^{163,164} The catalysts with the smallest iron-containing particles displayed a high catalytic activity but also exhibited a high methane selectivity. This result highlights the importance of selecting an optimum particle size for the design of active, selective, and stable catalyst for the production of lower olefins from synthesis gas. The catalysts prepared using inert supports showed a good combination of high catalytic activity with a high C₂–C₄ olefins selectivity and low methane formation as shown in Figure 12.

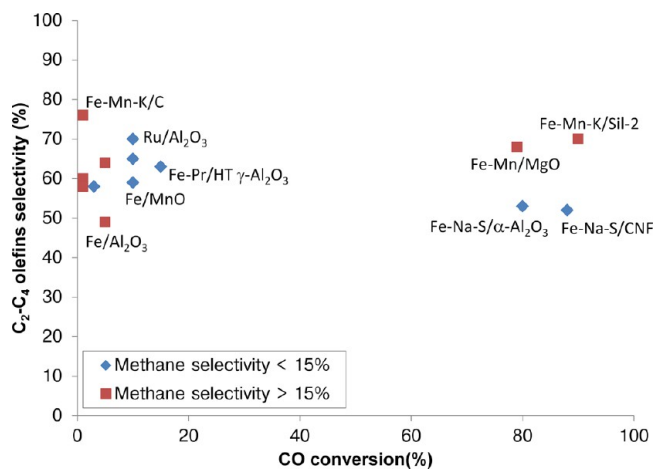


Figure 12. Supported catalysts for the FTO reaction (C₂–C₄ olefins selectivity >50%). Catalysts with CH₄ selectivities below 15%: diamonds.

Figure 12 shows that it is possible to obtain high C₂–C₄ olefins selectivities (>50%) with different formulations of supported Fe catalysts at low CO conversions. It is possible to achieve such high selectivities even with unpromoted catalysts because under these conditions secondary hydrogenation reactions are limited. The main challenge is to maintain the high C₂–C₄ selectivity at high CO conversion levels. From Figure 12 it is shown the Fe–Mn–K/Sil-2, Fe–Mn/MgO, and the Fe–Na–S catalysts prepared on inert supports displayed a high activity combined with high C₂–C₄ olefins selectivity. It is important to note that a methane selectivity of about 30% is expected when achieving a high C₂–C₄ olefins selectivity (~50%) according to the ASF distribution (Figure 8). From the

catalysts with high CO conversion and C₂–C₄ olefins selectivity, only the Na- and S-promoted catalysts showed methane selectivities below 20%.

Figure 13 displays lower olefins selectivity as a function of temperature for supported catalysts. This graph shows that high

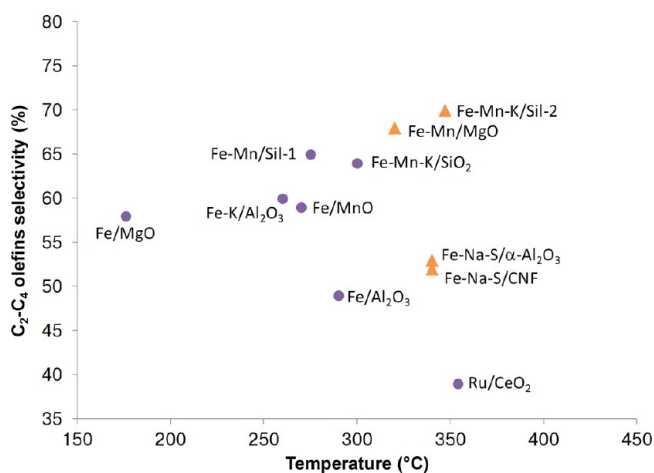


Figure 13. Selectivity to lower olefins as a function of temperature. Catalysts with light olefins selectivity higher than 35%. Catalysts with low CO conversion (<10%): circles. Catalysts with high CO conversion (>70%): triangles.

CO conversions can be achieved using high reaction temperatures (>300 °C). Under these conditions, the selectivity to shorter hydrocarbons is enhanced, increasing lower olefins selectivity but at the same time increasing methane production. The formation of carbon deposits is also favored at high reaction temperatures thus having a negative effect on catalytic activity. Carbon lay-down can be decreased by performing the reaction in the presence of H₂-rich syngas. Fe–Mn–K/Sil-2 and Fe–Mn/MgO showed a good catalytic performance when the reaction was carried out with a H₂/CO ratio of 2 whereas the Fe–Na–S catalysts supported on CNF or α-Al₂O₃ exhibited high activity even when using syngas with a H₂/CO ratio of 1.

3.2.6. Non-Fe-Based Supported Catalysts. Kou et al.¹⁶⁵ reported on gamma alumina supported zirconia catalyst for the production of ethylene from syngas. The catalyst exhibited a high selectivity to ethylene (70%) when the Fischer–Tropsch reaction was performed at 357 °C, 8 bar, and a H₂/CO ratio of 4.

Several Co-based catalyst have been proposed for the production of light olefins from synthesis gas.^{106,130,148,149,166,167} Feyzi et al.¹⁴⁸ prepared Co catalysts by precipitation in the presence of TiO₂. They investigated the catalytic performance under different reaction conditions and the promotion effects of Zn, K, Li, Rb, or Ce. The highest light olefins selectivity (47%) was obtained for a Co/TiO₂ catalyst promoted with 6 wt % Zn and tested at 240 °C and 1 bar.

Das et al.¹⁴⁹ reported on Co and Co–Mn supported catalysts prepared by impregnation of silicalite-1 with metal nitrates. A Co–Mn/sil-1 displayed a lower olefins selectivity of 33% when the reaction was performed at 275 °C, 21 bar, and H₂/CO ratio of 3. The addition of Mn to Co/sil-1 catalysts increased CO conversion only when the reaction was performed at 250 °C and not at higher temperatures. The modification with Mn slightly reduced the alkene selectivity, which is in contrast with results reported by other research groups.

A Co–Mo–K/SiO₂ catalyst was prepared by Chen et al.¹⁶⁷ using incipient wetness impregnation of cobalt nitrate, ammonium molybdate, and potassium carbonate. The catalyst was tested at 1 bar, 250–330 °C, and H₂/CO ratios ranging from 0.05 to 19. The introduction of Mo to the catalyst resulted in an improvement on the total O/P ratio (from 0.3 to 0.6), suppression of methane formation, and increase of chain growth probability. High light olefins selectivity on supported Mo-containing catalysts was also reported by Murchison.⁸²

High selectivities to light olefins have been also reported for Ru-based catalysts supported on titania,^{150,151} alumina,¹⁵² CeO₂,¹⁵³ and Nb₂O₅.¹⁵⁴ However, these high C₂–C₄ olefins selectivities have only been obtained at low CO conversions (Table 4).

4. OUTLOOK

The growing interest of different countries to secure their supply of C₂–C₄ olefins will continue to drive research and development of catalysts and processes for the production of these important commodity chemicals from non-oil-based feedstocks. The indirect processes, MTO and DMTO, are already industrially applied for the production of lower olefins from synthesis gas. These processes display high selectivities to ethylene and propylene and could be an attractive option for supplying the polymers industry with feedstocks. The MTO and DMTO processes require hydrogen-rich syngas as for the preceding methanol synthesis. For this reason, MTO and DMTO are suitable options using natural gas as feed. In the case of CO-rich syngas, produced by gasification of coal or biomass, an additional step for the adjustment of the H₂/CO ratio is required by means of the water gas shift reaction. Additionally, coal or biomass-based syngas contains sulfur and other contaminants that act as strong poisons for the catalysts used in the synthesis of methanol and DME. This implies that stringent, and costly, gas cleanup procedures should be used for the conditioning of CO-rich syngas intended to be used in the methanol synthesis process. Also, research is needed to improve the activity, selectivity, and stability of MTO and DMTO catalysts as most of them exhibit fast deactivation due to the formation of carbon deposits.

The FTO process is a direct route that offers feedstock flexibility. When iron-based catalysts are used, the process can be performed using CO-rich syngas directly, without any H₂/CO ratio adjustment, in view of their high water gas shift activity. Iron is more robust than other metals and can withstand some contaminants present in coal or biomass-based syngas. In fact, it is shown from this review that iron can be even more selective to light olefins in the presence of low concentrations of sulfur.

The FTO process displays lower ethylene and propylene selectivities in comparison to MTO or DMTO. However, FTO could be an attractive route to supply chemical complexes where the byproducts, i.e., C₅₊ and oxygenates, could be utilized. In view of limited availability of the composition of the C₂–C₄ olefin fraction we are not able to make a detailed assessment of FTO versus MTO.

The development of catalytic processes for the conversion of CO₂ into olefins might gain importance in the future as an alternative pathway for light olefins production.^{168–175} The environmental impact of FTO might be further reduced using CO₂ and “solar” hydrogen as feedstock.

The FTO route becomes more feasible with every improvement on activity, selectivity, and stability of the catalytic system.

Iron can be presented as the metal of choice for the FTO reaction as it is inexpensive, it is highly selective toward olefins, and it is possible to achieve methane selectivities below the prediction of the ASF product distribution. The design of effective iron-based catalysts for the selective production of light olefins involves several factors:

- The selection of a support that enables the formation of the active phase and its intimate contact with the chemical promoters
- The adequate choice of promoters to increase the selectivity to light olefins and minimize methane production
- The use of preparation methods that allow obtaining a homogeneous spatial distribution of iron-containing particles with narrow size distribution in the optimum size range
- The selection of optimum process conditions to maximize the catalyst life without compromising product selectivity

The application of FTO is subject to economical and technical feasibility studies and to the development of optimum catalysts and production processes. The selection of a process for the production of lower olefins depends not only on capital and operational costs but also on the feedstocks available and the product slate.

■ AUTHOR INFORMATION

Corresponding Author

*E-mail: K.P.deJong@uu.nl.

Notes

The authors declare no competing financial interest.

■ REFERENCES

- (1) McCoy, M., Ed. *Chem. Eng. News* **2011**, *89*, 55–56.
- (2) Wittcoff, H. A.; Reuben, B. G.; Plotkin, J. S. *Industrial Organic Chemicals*, 2nd ed.; John Wiley and Sons, Inc.: Hoboken, NJ, 2004; 662 pp.
- (3) Association of Petrochemicals Producers in Europe. West European Market Review 2010. <http://www.petrochemistry.net>.
- (4) Nexant Inc. CHEMSYSTEMS PERP program “Propylene”; Rep. No. PERP 06/07-3; 2008. <http://www.chemsystems.com>.
- (5) Tallman, M. J.; Klavers, R. North American olefin producers riding the shale gas wave; 2013 (April 1). <http://www.hydrocarbonprocessing.com/>.
- (6) Bowen, C. P.; Jones, D. *Hydrocarbon Process.* **2008**, No. April, 71–79.
- (7) International Energy Agency (IEA). Energy technology transitions for industry; OECD/IEA: Paris, France, 2009. <http://www.iea.org>.
- (8) Pyl, S. P.; Schietekat, C. M.; Reyniers, M.; Abhari, R.; Marin, G. B.; van Geem, K. M. *Chem. Eng. J.* **2011**, *176–177*, 178–187.
- (9) International Energy Agency (IEA). World Energy Outlook; OECD/IEA: Paris, France, 2010). <http://www.iea.org>.
- (10) International Energy Agency (IEA). Technology roadmap. Biofuels for transportation; OECD/IEA: Paris, France, 2011. <http://www.iea.org>.
- (11) Stöcker, M. *Angew. Chem., Int. Ed.* **2008**, *47*, 9200–9211.
- (12) Ragauskas, A. J.; Williams, C. K.; Davison, B. H.; Britovsek, G.; Cairney, J.; Keckert, C. A.; Frederick, W. J., Jr.; Hallett, J. P.; Leak, D. J.; Liotta, C. L.; Mielenz, J. R.; Murphy, R.; Templar, R.; Tschaplinski, T. *Science* **2006**, *311*, 484–489.
- (13) Brown, R. C., Ed. *Thermochemical processing of biomass: conversion into fuels, chemicals, and power*, 1st ed.; John Wiley & Sons, Ltd.: Chichester, U.K., 2011; 350 pp.

- (14) Faaij, A. P. C. *Mitigation Adapt. Strategies Global Change* **2006**, *11*, 343–375.
- (15) Tijmensen, M. J. A.; Faaij, A. P. C.; Hamelinck, C. N.; van Hardeveld, M. R. M. *Biomass Bioenerg.* **2002**, *23*, 129–152.
- (16) U.S. Energy Information Administration (EIA). Summary: U.S. crude oil, natural gas, and natural gas liquid proved reserves 2009; U.S. Energy Information Administration: Washington, DC, 2010. <http://www.eia.gov>.
- (17) U.S. Energy Information Administration (EIA). International Energy Outlook 2011; Rep. No. DOE/EIA-0484(2011); U.S. Energy Information Administration: Washington, DC, 2011. <http://www.eia.gov>.
- (18) Jenkins, S. *Chem. Eng.* **2012**, No. October, 17–19.
- (19) McDonald, P. *Oil Energy Trends* **2013**, *38*, 10–17.
- (20) International Energy Agency (IEA). Golden rules for a golden age of gas. World energy outlook. Special report on unconventional gas; OECD/IEA: Paris, France, 2012. <http://www.iea.org>.
- (21) Hughes, J. D. *Nature* **2013**, *494*, 307–308.
- (22) Liu, Z.; Sun, C.; Wang, G.; Wang, Q.; Cai, G. *Fuel Process. Technol.* **2000**, *62*, 161–172.
- (23) Wang, C.; Wang, Q.; Sun, X.; Xu, L. *Catal. Lett.* **2005**, *105*, 93–101.
- (24) Wang, C.; Xu, L.; Wang, Q. *J. Nat. Gas Chem.* **2003**, *12*, 10–16.
- (25) Janardanarao, M. *Ind. Eng. Chem. Res.* **1990**, *29*, 1735–1753.
- (26) Lunsford, J. H. *Catal. Today* **2000**, *63*, 165–174.
- (27) Chen, D.; Moljord, K.; Holmen, A. *Microporous Mesoporous Mater.* **2012**, *164*, 239–250.
- (28) Zhao, T. S.; Takemoto, T.; Tsubaki, N. *Catal. Comm.* **2006**, *7*, 647–650.
- (29) Čejka, J.; Corma, A.; Zones, S., Eds. *Zeolites and Catalysis. Synthesis, reactions and applications*, 1st ed.; Wiley-VCH Verlag GmbH & Co. KGaA: Weinheim, Germany, 2010; 1056 pp.
- (30) Cai, G.; Liu, Z.; Shi, R.; He, C.; Yang, L.; Sun, C.; Chang, Y. *Appl. Catal., A* **1995**, *125*, 29–38.
- (31) Knifton, J. F. *J. Catal.* **1983**, *79*, 147–155.
- (32) Dupain, X.; Krul, R. A.; Schaverien, C. J.; Makkee, M.; Moulijn, J. A. *Appl. Catal., B* **2006**, *63*, 277–295.
- (33) Traa, Y. *Chem. Commun.* **2010**, *46*, 2175.
- (34) Schwab, E.; Weck, A.; Steiner, J.; Bay, K. *Oil Gas Eur. Mag.* **2010**, *1*, 44–47.
- (35) Snel, R. *Catal. Rev. Sci. Eng.* **1987**, *29*, 361–445.
- (36) Literature survey on patents and scientific articles in the CAS database using the keywords “Fischer–Tropsch”, “CO hydrogenation”, and “lower olefins”.
- (37) BP Statistical Review of World Energy June 2012. <http://www.bp.com/statisticalreview>.
- (38) Steynberg, A. P.; Dry, M. E., Eds. *Fischer–Tropsch Technology*; Series: Studies in surface science and catalysis No. 152; Elsevier: Amsterdam, 2004.
- (39) Arakawa, H.; Kiyozumi, Y.; Suzuki, K.; Takeuchi, K.; Matsuzaki, T.; Sugi, Y.; Fukushima, T.; Matsushita, S. *Chem. Lett.* **1986**, 1341–1342.
- (40) Denise, B.; Sneed, R. P. A. *Appl. Catal.* **1986**, *27*, 107–116.
- (41) Park, J. Y.; Lee, Y. J.; Jun, K. W.; Bae, J. W.; Viswanadham, N.; Kim, Y. H. *J. Ind. Eng. Chem.* **2009**, *15*, 847–853.
- (42) Lee, Y. J.; Park, J. Y.; Jun, K. W.; Bae, J. W.; Viswanadham, N. *Catal. Lett.* **2008**, *126*, 149–154.
- (43) Abelló, S.; Montané, D. *ChemSusChem* **2011**, *4*, 1538–1556.
- (44) de Klerk, A. *Fischer–Tropsch refining*; Wiley-VCH Verlag and Co., KGaA: Weinheim, Germany, 2011; 638 pp.
- (45) van der Laan, G. P.; Beenackers, A. A. C. M. *Catal. Rev.* **1999**, *41*, 255–318.
- (46) Dry, M. E. *Catal. Today* **2002**, *71*, 227–241.
- (47) Zhang, Q.; Kang, J.; Wang, Y. *ChemCatChem* **2010**, *2*, 1030–1058.
- (48) Zhang, Q.; Deng, W.; Wang, Y. *J. Energy Chem.* **2013**, *22*, 27–38.
- (49) Sun, B.; Xu, K.; Nguyen, L.; Qiao, M.; Tao, F. *ChemCatChem* **2012**, *4*, 1498.
- (50) de Smit, E.; Weckhuysen, B. M. *Chem. Soc. Rev.* **2008**, *37*, 2758.
- (51) Iglesia, E. *Appl. Catal., A* **1997**, *161*, 59–78.
- (52) Khodakov, A. Y.; Chu, W.; Fongarland, P. *Chem. Rev.* **2007**, *107*, 1692–1744.
- (53) Tsakoumis, N. E.; Rønning, M.; Borg, Ø.; Rytter, E.; Holmen, A. *Catal. Today* **2010**, *154*, 162–182.
- (54) Enger, B. C.; Holmen, A. *Catal. Rev. Sci. Eng.* **2012**, *54*, 437–488.
- (55) Torres Galvis, H. M.; Bitter, J. H.; Khare, C. B.; Ruitenbeek, M.; Dugulan, A. I.; de Jong, K. P. *Science* **2012**, *335*, 835–838.
- (56) Torres Galvis, H. M.; Koeken, A. C. J.; Bitter, J. H.; Davidian, T.; Ruitenbeek, M.; Dugulan, A. I.; de Jong, K. P. *J. Catal.* **2013**, *303*, 22–30.
- (57) Dry, M. E.; Erasmus, H. B. de W. *Annu. Rev. Energy* **1987**, *12*, 1–21.
- (58) Büssemeier, B.; Frohning, C. D.; Cornils, B. *Hydrocarbon Process.* **1976**, *56*, 105–112.
- (59) Büssemeier, B.; Frohning, C. D.; Kluy, W. DE Patent 2518964, 1976.
- (60) Büssemeier, B.; Frohning, C. D.; Horn, G.; Kluy, W. US Patent 4,564,642, 1986.
- (61) Roy, S. C.; Prasad, H. L.; Dutta, P.; Bhattacharya, A.; Singh, B.; Kumar, S.; Maharaj, S.; Kaushik, V. K.; Pillai, S. M.; Ravidranathan, M. *Appl. Catal., A* **2001**, *220*, 153–164.
- (62) Goldwasser, M. R.; Dorantes, V. E.; Pérez-Zurita, M. J.; Sojo, P. R.; Cubeiro, M. L.; Pietri, E.; González-Jiménez, F.; Lee, Y. N.; Moronta, D. *J. Mol. Catal. A* **2003**, *193*, 227–236.
- (63) Sağlam, M. *Ind. Eng. Chem. Res.* **1989**, *28*, 150–154.
- (64) Kang, S. H.; Bae, J. W.; Prasad, P. S. S.; Park, S. J.; Woo, K. J.; Jun, K. W. *Catal. Lett.* **2009**, *130*, 630–636.
- (65) Vielstich, W.; Kitzelmann, D. GB Patent 2050859, 1981.
- (66) Hoffer, B. W.; Bunzel, S.; Neumann, D.; Bay, K.; Schwab, E.; Grässle, U.; Steiner, J. International Patent Application No. WO2009013174, 2009.
- (67) Tihay, F.; Roger, A. C.; Kiennemann, A.; Pourroy, G. *Catal. Today* **2000**, *58*, 263–269.
- (68) Tihay, F.; Pourroy, G.; Richard-Plouet, M.; Roger, A. C.; Kiennemann, A. *Appl. Catal., A* **2001**, *206*, 29–42.
- (69) van Dijk, W. L.; Niemantsverdriet, J. W.; van der Kraan, A. M.; van der Baan, H. S. *Appl. Catal.* **1982**, *2*, 273–288.
- (70) Crous, R.; Bromfield, T. C.; Booyens, S. International Patent Application No. WO2010066386, 2010.
- (71) Hadadzadeh, H.; Mirzaei, A. A.; Morshedi, M.; Raeisi, A.; Feyzi, M.; Rostamizadeh, N. *Petrol. Chem.* **2010**, *50*, 78–86.
- (72) González-Cortés, S. L.; Rodulfo-Baechler, S. M. A.; Oliveros, A.; Orozco, J.; Fontal, B.; Mora, A. J.; Delgado, G. *React. Kinet. Catal. Lett.* **2002**, *75*, 3–12.
- (73) Mirzaei, A. A.; Habibpour, R.; Kashi, E. *Appl. Catal., A* **2005**, *296*, 222–231.
- (74) Feyzi, M.; Hassankhani, A. *J. Nat. Gas Chem.* **2011**, *20*, 677–686.
- (75) Kölbl, H.; Tillmetz, K. D. US Patent 4177203, 1979.
- (76) Deckwer, W. D.; Serpemen, Y.; Ralek, M.; Schmidt, B. *Ind. Eng. Chem. Process. Des. Dev.* **1982**, *21*, 222–231.
- (77) Soled, S. L.; Fiato, R. A., GB Patent 2152072A, 1985.
- (78) Hutchings, G. J.; Boeyens, J. C. A. *J. Catal.* **1986**, *100*, 507–511.
- (79) Copperthwaite, R. G.; Hutchings, G. J.; van der Riet, M.; Woodhouse, J. *Ind. Eng. Chem. Res.* **1987**, *26*, 869–874.
- (80) Zhang, J.; Fan, S.; Zhao, T. S.; Li, W.; Sun, Y. *React. Kinet. Mech. Cat.* **2011**, *102*, 437–445.
- (81) Sano, T.; Yanagisawa, H.; Saito, K.; Okabe, K.; Okado, H.; Takaya, H.; Bando, K. *Appl. Catal.* **1985**, *19*, 247–258.
- (82) Murchison, C. B.; Murdick, D. A. US Patent 4199522, 1980.
- (83) Arai, T.; Maruya, K.; Domen, K.; Onishi, T. *J. Chem. Soc., Chem. Commun.* **1987**, *23*, 1757–1758.
- (84) Kojima, I.; Miyazaki, E.; Yasumori, I. *J. Chem. Soc., Chem. Commun.* **1980**, *12*, 573–574.
- (85) Park, K. Y.; Seo, W. K.; Lee, J. S. *Catal. Lett.* **1991**, *11*, 349–356.

- (86) Mirzaei, A. A.; Galavy, M.; Beigbabaei, A.; Eslamimanes, V. J. *Iran. Chem. Soc.* **2007**, *4*, 347–363.
- (87) Costa, J. L.; Noels, A. F.; Demonceau, A.; Hubert, A. J. *J. Catal.* **1987**, *105*, 1–9.
- (88) Yao, J.; Kimble, J. B. US Patent 2007043127 A1, 2007.
- (89) Venter, J.; Kaminsky, M.; Geoffroy, G. L.; Vannice, M. A. *J. Catal.* **1987**, *103*, 450–465.
- (90) Venter, J.; Kaminsky, M.; Geoffroy, G. L.; Vannice, M. A. *J. Catal.* **1987**, *105*, 155–162.
- (91) Anderson, J. R.; Boudart, M., Eds. *Catalysis: Science and Technology*; Springer-Verlag: New York, 1981.
- (92) Dry, M. E.; Oosthuizen, G. J. *J. Catal.* **1968**, *11*, 18–24.
- (93) Yang, Y.; Xiang, H. W.; Xu, Y. Y.; Bai, L.; Li, Y. W. *Appl. Catal., A* **2004**, *266*, 181.
- (94) Lohitharn, N.; Goodwin, J. G. *J. Catal.* **2008**, *260*, 7.
- (95) Rankin, J. L.; Bartholomew, C. H. *J. Catal.* **1986**, *100*, 533.
- (96) Ribeiro, M. C.; Jacobs, G.; Davis, B. H.; Cronauer, D., C.; Kropf, A. J.; Marshall, C. L. *J. Phys. Chem. C* **2010**, *114*, 7895–7903.
- (97) An, X.; Wu, B. S.; Wan, H. J.; Li, T. Z.; Tao, Z. C.; Xiang, H. W.; Li, Y. W. *Catal. Commun.* **2007**, *8*, 1957–1962.
- (98) Kalakkad, D. S.; Shroff, M. D.; Köhler, S. D.; Jackson, N. B.; Datye, A. K. *Appl. Catal., A* **1995**, *133*, 335–350.
- (99) Bromfield, T. C.; Coville, N. J. *Appl. Catal., A* **1999**, *186*, 297–307.
- (100) Bromfield, T. C.; Coville, N. J. *Appl. Surf. Sci.* **1997**, *119*, 19–24.
- (101) Wu, B.; Bai, L.; Xiang, H.; Li, Y.; Zhang, Z.; Zhong, B. *Fuel* **2004**, *83*, 205–212.
- (102) Kritzinger, J. A. *Catal. Today* **2002**, *71*, 307–318.
- (103) Malessa, R.; Baerns, M. *Ind. Eng. Chem. Res.* **1988**, *27*, 279–283.
- (104) Cooper, M. E.; Frost, J. *Appl. Catal.* **1990**, *57*, L5–L8.
- (105) Blanchard, M.; Vanhove, D.; Petit, F.; Mortreux, A. *J. Chem. Soc., Chem. Commun.* **1980**, *19*, 908–909.
- (106) Peters, K. GB Patent 833976, 1960.
- (107) Mirzaei, A. A.; Faizi, M.; Habibpour, R. *Appl. Catal., A* **2006**, *306*, 98–107.
- (108) Shroff, M. D.; Kalakkad, D. S.; Coulter, K. E.; Köhler, S. D.; Harrington, M. S.; Jackson, N. B.; Sault, A. G.; Datye, A. K. *J. Catal.* **1995**, *156*, 185–207.
- (109) Bukur, D. B.; Ma, W. P.; Carreto-Vazquez, V. *Top. Catal.* **2005**, *32*, 135–141.
- (110) Jager, B.; Espinoza, R. *Catal. Today* **1995**, *23*, 17–28.
- (111) de Smit, E.; Cinquini, F.; Beale, A. M.; Safonova, O. V.; van Beek, W.; Sautet, P.; Weckhuysen, B. M. *J. Am. Chem. Soc.* **2010**, *132*, 14928–14941.
- (112) de Smit, E.; Swart, I.; Creemer, J. F.; Hoveling, G. H.; Gilles, M. K.; Tyliczszak, T.; Kooyman, P. J.; Zandbergen, H. W.; Morin, C.; Weckhuysen, B. M.; de Groot, F. M. F. *Nature* **2008**, *456*, 222–225.
- (113) Gonzalez-Jimenez, I. D.; Cats, K.; Davidian, T.; Ruitenbeek, M.; Meirer, F.; Liu, Y.; Nelson, J.; Andrews, J. C.; Pianetta, P.; de Groot, F. M. F.; Weckhuysen, B. M. *Angew. Chem., Int. Ed.* **2012**, *51*, 11986–11990.
- (114) Torres Galvis, H. M.; Koeken, A. C. J.; Bitter, J. H.; Davidian, T.; Ruitenbeek, M.; Dugulan, A. I.; de Jong, K. P. *Catal. Today* **2013**, DOI: 10.1016/j.cattod.2013.03.018.
- (115) Park, J. Y.; Lee, Y. J.; Khanna, P. K.; Jun, K. W.; Bae, J. W.; Kim, Y. H. *J. Mol. Catal. A* **2010**, *323*, 84–90.
- (116) Perrichon, V.; Charcosset, H.; Barrault, J.; Forquy, C. *Appl. Catal.* **1983**, *7*, 21–29.
- (117) Rao, K. R. P. M.; Huggins, F. E.; Mahajan, V.; Huffman, G. P.; Rao, V. U. S.; Bhatt, B. L.; Bukur, D. B.; Davis, B. H.; O'Brien, R. J. *Top. Catal.* **1995**, *2*, 71–78.
- (118) Zhang, C. H.; Wan, H. J.; Yang, Y.; Xiang, H. W.; Li, Y. W. *Catal. Commun.* **2006**, *7*, 733–738.
- (119) Suo, H.; Wang, S.; Zhang, C. H.; Xu, J.; Wu, B. S.; Yang, Y.; Xiang, H. W.; Li, Y. W. *J. Catal.* **2012**, *286*, 111–123.
- (120) Bruce, L.; Hope, G.; Turney, T. W. *React. Kinet. Catal. Lett.* **1982**, *20*, 175–180.
- (121) Commereuc, D.; Chauvin, Y. *J. Chem. Soc., Chem. Commun.* **1980**, *4*, 154–155.
- (122) Stoop, F.; van der Wiele, K. *Appl. Catal.* **1986**, *23*, 35–47.
- (123) Jiang, N.; Yang, G.; Zhang, X.; Wang, L.; Shi, C.; Tsubaki, N. *Catal. Commun.* **2011**, *12*, 951–954.
- (124) Baker, B. G.; Clark, N. J. *Stud. Surf. Sci. Catal.* **1987**, *31*, 455–465.
- (125) Baker, B. G.; Clark, N. J.; Macarthur, H.; Summerville, E. International Patent Application No. WO8400702, 1984.
- (126) Basset, J.; Chauvin, Y.; Commereuc, D.; Smith, A.; Theolier, A. FR Patent 2391978, 1977.
- (127) Barrault, J.; Forquy, C.; Menezo, J. C.; Maurel, R. *React. Kinet. Catal. Lett.* **1980**, *15*, 153–158.
- (128) Arakawa, H.; Bell, A. T. *Ind. Eng. Chem. Process. Des. Dev.* **1983**, *22*, 97–103.
- (129) Barrault, J.; Forquy, C.; Perrichon, V. *J. Mol. Catal.* **1982**, *17*, 195–202.
- (130) Barrault, J.; Forquy, C.; Perrichon, V. *Appl. Catal.* **1983**, *5*, 119–125.
- (131) Rao, V. U. S.; Gormley, R. J. US Patent 4,340,503, 1982.
- (132) Bae, J. W.; Kang, S. H.; Lee, Y. J.; Jun, K. W. International Patent Application No. WO 2009051353, 2009.
- (133) Kang, S. H.; Bae, J. W.; Prasad, P. S. S.; Jun, K. W. *Catal. Lett.* **2008**, *125*, 264–270.
- (134) Xu, L.; Wang, Q.; Xu, Y.; Huang, J. *Catal. Lett.* **1995**, *31*, 253–266.
- (135) Das, D.; Ravichandran, G.; Chakrabarty, D. K. *Catal. Today* **1997**, *36*, 285–293.
- (136) Kang, S. H.; Bae, J. W.; Woo, K. J.; Prasad, P. S. S.; Jun, K. W. *Fuel Process. Technol.* **2010**, *91*, 399–403.
- (137) Mitsudo, T.; Boku, H.; Murachi, S.; Ishihara, A.; Watanabe, Y. *Chem. Lett.* **1985**, 1463–1466.
- (138) Gustafson, B. L. US Patent 4518714, 1985.
- (139) Xu, L.; Wang, Q.; Xu, Y.; Huang, J. *Catal. Lett.* **1994**, *24*, 177–185.
- (140) Hugues, F.; Besson, B.; Basset, J. M. *J. Chem. Soc., Chem. Commun.* **1980**, *15*, 719–721.
- (141) Barrault, J.; Renard, C. *Appl. Catal.* **1985**, *14*, 133–143.
- (142) Barrault, J.; Zivkov, C.; Bergaya, F.; Gatineau, L.; Hassoun, N.; van Damme, H.; Mari, D. *J. Chem. Soc., Chem. Commun.* **1988**, *21*, 1403–1404.
- (143) Schulte, H. J.; Graf, B.; Xia, W.; Muhler, M. *ChemCatChem* **2012**, *4*, 350–355.
- (144) Barrault, J.; Renard, C. FR Patent 2571274, 1984.
- (145) Yang, Z.; Pan, X.; Wang, J.; Bao, X. *Catal. Today* **2012**, *186*, 121–127.
- (146) Sommen, A. P. B.; Stoop, F.; van der Wiele, K. *Appl. Catal.* **1985**, *14*, 277–288.
- (147) Jung, H. J.; Walker, P. L., Jr.; Vannice, M. A. *J. Catal.* **1982**, *75*, 416–422.
- (148) Feyzi, M.; Khodaei, M. M.; Shahmoradi, J. *Fuel Process. Technol.* **2012**, *93*, 90–98.
- (149) Das, D.; Ravichandran, G.; Chakrabarty, D. K. *Appl. Catal., A* **1995**, *131*, 335–345.
- (150) Vannice, M. A.; Garten, R. L. *J. Catal.* **1980**, *63*, 255–260.
- (151) Doi, Y.; Miyake, H.; Yokota, A.; Soga, K. *J. Catal.* **1985**, *95*, 293–295.
- (152) Okuhara, T.; Kobayashi, K.; Kimura, T.; Misono, M.; Yoneda, Y. *J. Chem. Soc., Chem. Commun.* **1981**, *21*, 1114–1115.
- (153) Pierantozzi, R. GB Patent 2119277, 1983.
- (154) Vannice, M. A.; Tauster, S. J. GB Patent 2006261, 1979.
- (155) van Dillen, A. J.; Terörde, R. J. A. M.; Lensveld, D. J.; Geus, J. W.; de Jong, K. P. *J. Catal.* **2003**, *216*, 257–264.
- (156) Yeh, E. B.; Schwartz, L. H.; Butt, J. B. *J. Catal.* **1985**, *91*, 241–253.
- (157) Koeken, A. C. J.; Torres Galvis, H. M.; Davidian, T.; Ruitenbeek, M.; de Jong, K. P. *Angew. Chem., Int. Ed.* **2012**, *51*, 7190–7193.

- (158) Cubeiro, M. L.; López, C. M.; Colmenares, A.; Texeira, L.; Goldwasser, M. R.; Pérez Zurita, M. J.; Machado, F.; González Jiménez, F. *Appl. Catal., A* **1998**, *167*, 183–193.
- (159) de Jong, K. P.; Geus, J. W. *Catal. Rev. Sci. Eng.* **2000**, *42*, 481–510.
- (160) Jüntgen, H. *Fuel* **1986**, *65*, 1436–1446.
- (161) Jones, V. K.; Neubauer, L. R.; Bartholomew, C. H. *J. Phys. Chem.* **1986**, *90*, 4832–4839.
- (162) Torres Galvis, H. M.; Bitter, J. H.; Davidian, T.; Ruitenbeek, M.; Dugulan, A. I.; de Jong, K. P. *J. Am. Chem. Soc.* **2012**, *134*, 16207–16215.
- (163) Bezemer, G. L.; Bitter, J. H.; Kuipers, H. P. C. E.; Oosterbeek, H.; Holeyijn, J. E.; Xu, X.; Kapteijn, F.; van Dillen, A. J.; de Jong, K. P. *J. Am. Chem. Soc.* **2006**, *128*, 3956–3964.
- (164) den Breejen, J. P.; Radstake, P. B.; Bezemer, G. L.; Bitter, J. H.; Frøseth, V.; Holmen, A.; de Jong, K. P. *J. Am. Chem. Soc.* **2009**, *131*, 7197–7203.
- (165) Kou, Y.; Su, G. Q.; Zhang, W. Z.; Yin, Y. Q. *J. Catal.* **1996**, *162*, 361–364.
- (166) Fraenkel, D.; Gates, B. C. *J. Am. Chem. Soc.* **1980**, *102*, 2478–2480.
- (167) Chen, H.; Adesina, A. A. *Appl. Catal., A* **1994**, *112*, 87–103.
- (168) Prasad, P. S. S.; Bae, J. W.; Jun, K. W.; Lee, K. W. *Catal. Surv. Asia* **2008**, *12*, 170–183.
- (169) Riedel, T.; Schulz, H.; Schaub, G.; Jun, K. W.; Hwang, J. S.; Lee, K. W. *Top. Catal.* **2003**, *26*, 41–54.
- (170) Riedel, T.; Claeys, M.; Schulz, H.; Schaub, G.; Nam, S. S.; Jun, K. W.; Choi, M. J.; Kishan, G.; Lee, K. W. *Appl. Catal., A* **1999**, *186*, 201–213.
- (171) Wang, J.; You, Z.; Zhang, Q.; Deng, W.; Wang, Y. *Catal. Today* **2013**, DOI: 10.1016/j.cattod.2013.03.031.
- (172) Wang, W.; Wang, S.; Ma, X.; Gong, J. *Chem. Soc. Rev.* **2011**, *40*, 3703–3727.
- (173) Moreno-Castilla, C.; Salas-Peregrin, M.; López-Garzón, F. J. *Fuel* **1995**, *74*, 830–835.
- (174) Yao, Y.; Liu, X.; Hildebrandt, D.; Glasser, D. *Appl. Catal., A* **2012**, *433–434*, 58–68.
- (175) Hu, B.; Frueh, S.; Garces, H. F.; Zhang, L.; Aindow, M.; Brooks, C.; Kreidler, E.; Suib, S. L. *Appl. Catal., B* **2013**, *132–133*, 54–61.